



Scholars' Mine

Masters Theses

Student Theses and Dissertations

Summer 2017

Study of surface complexation and mineral dissolution during water-rock interaction in high salinity waterflooding at elevated temperatures

Sameer Salasakar

Follow this and additional works at: https://scholarsmine.mst.edu/masters_theses

 Part of the [Oil, Gas, and Energy Commons](#), and the [Petroleum Engineering Commons](#)

Department:

Recommended Citation

Salasakar, Sameer, "Study of surface complexation and mineral dissolution during water-rock interaction in high salinity waterflooding at elevated temperatures" (2017). *Masters Theses*. 7692.
https://scholarsmine.mst.edu/masters_theses/7692

This Thesis - Open Access is brought to you for free and open access by Scholars' Mine. It has been accepted for inclusion in Masters Theses by an authorized administrator of Scholars' Mine. This work is protected by U. S. Copyright Law. Unauthorized use including reproduction for redistribution requires the permission of the copyright holder. For more information, please contact scholarsmine@mst.edu.

STUDY OF SURFACE COMPLEXATION AND MINERAL
DISSOLUTION DURING WATER-ROCK INTERACTION IN HIGH
SALINITY WATERFLOODING AT ELEVATED TEMPERATURES

by

SAMEER SALASAKAR

A THESIS

Presented to the Faculty of the Graduate School of the
MISSOURI UNIVERSITY OF SCIENCE AND TECHNOLOGY

In Partial Fulfillment of the Requirements for the Degree

MASTER OF SCIENCE IN PETROLEUM ENGINEERING

2017

Approved by

Dr. Peyman Heidari, Advisor
Dr. Shari Dunn-Norman
Dr. Ralph Flori

ABSTRACT

High salinity waterflooding for carbonate reservoirs is efficient and cheap method used for improved oil recovery. Various mechanisms have been proposed including adsorption/desorption on rock surface, mineral dissolution and precipitation, multicomponent ion exchange, interfacial tension reduction, fine migration and double layer expansion. These all process alter the wettability which leads to improved oil recovery.

Objective of this study was to understand processes that occur during water-rock interaction when high salinity water is flooded into the reservoir. In this work, effect of temperature on water-rock interaction is studied along with effect of pH and specific surface areas of calcite at normal and elevated temperatures. To understand processes occurring on surface of rock, reactive transport model for brine-rock interaction was developed. It included surface complexation and mineral dissolution processes which contribute towards wettability alteration. Effect of pH, specific surface area of calcite on surface complexation and mineral dissolution at normal and elevated temperatures showed that rate of mineral dissolution was higher than surface complexation reactions. Calcite dissolved volumes for varied composition of injected brine were compared with oil recovery percentages. The results showed that calcite dissolution increased with increase in oil recovery at higher temperatures. The study showed that improved oil recovery is complicated process which is result of various processes and steps involved. Sensitivity of each process and step for wettability alteration can be different depending on environment

ACKNOWLEDGEMENTS

I would like to express sincere gratitude to my advisor, Dr. Peyman Heidari, for his guidance, supervision, time and funding. This thesis was made possible by his patience, persistence and provision of outstanding environment for research. It has been honor to be his student. I would also like to thank my committee members, Dr. Shari Dunn-Norman and Dr. Ralph Flori.

Also, I would like to thank all of my group mates: Hasan Al-Saedi, Hector Donoso, Mahta Ansari, Kelsi Leverett, Pu Han, and Yao Wang for their help to make this work possible.

I would like to acknowledge the Missouri University of Science and Technology and Geosciences, geological and petroleum engineering department for providing great working environment and their support.

At the end, I would also like to thank my parents and friends for supporting me in every endeavor.

TABLE OF CONTENTS

	Page
ABSTRACT	iii
ACKNOWLEDGEMENTS	iv
LIST OF ILLUSTRATIONS.....	vii
LIST OF TABLES	ix
NOMENCLATURE.....	x
SECTION	
1 INTRODUCTION.....	1
1.1 OIL RECOVERY METHODS	2
1.1.1 Primary Oil Recovery Methods	3
1.1.2 Secondary Oil Recovery Methods.....	4
1.1.3 Tertiary Oil Recovery Methods	5
1.2 BRINE COMPOSITION AND WATERFLOODING EFFICIENCY	9
1.3 WETTABILITY.....	13
1.4 FACTORS AFFECTING WETTABILITY OF ROCK	20
1.5 OBJECTIVE	27
2 METHODOLOGY	28
2.1 REACTIVE TRANSPORT	28
2.2 REACTIONS	30

3	RESULTS AND DISCUSSION	33
3.1	BASE CASE SIMULATIONS	33
3.2	CHEMICAL ANALYSIS	35
3.3	SURFACE COMPLEXES	37
3.4	EFFECT OF VARYING TEMPERATURE	39
3.5	BRINE COMPOSITION AND CALCITE DISSOLUTION	48
4	CONCLUSION AND RECOMMENDATION	50
4.1	CONCLUSION	50
4.2	RECOMMENDATIONS	51
	BILBIOGRAPHY	52
	VITA	56

LIST OF ILLUSTRATIONS

	Page
Fig 1.1. Production phases.	3
Fig 1.2. EOR methods by lithology.	7
Fig 1.3. Oil recovery by spontaneous imbibition.....	10
Fig 1.4. Oil recovery by spontaneous imbibition.....	11
Fig 1.5. Flooding system.....	12
Fig 1.6. Effect of rock wettability on oil-water relative permeabilities.....	15
Fig 1.7. The interfacial tension values and contact angle.....	16
Fig 1.8. Idealized representation of water-wet and oil-wet reservoir rocks.....	17
Fig 1.9. Dependence of oil saturation on wettability.....	18
Fig 1.10. Wetting conditions on solid.....	19
Fig 1.11. SEM image of carbonate section.	22
Fig 1.12. Spontaneous imbibition into chalk cores saturated with different oils.	22
Fig 1.13. Capillary pressure diagram used to characterize wettability.	23
Fig 1.14. Maximum oil recovery from chalk cores at 100 and 130°C	24
Fig 1.15. Suggested chemical mechanism for wettability alteration.....	25
Fig 1.16. Competitive adsorption of Ca^{2+} and Mg^{2+} at room temperature	26
Fig 1.17. Competitive adsorption of Ca^{2+} and Mg^{2+} at 130°C	27
Fig 2.1. Dimensions of chalk core.....	29
Fig 3.1. Concentrations of effluent Ca^{2+} , Mg^{2+} and SCN^-	35
Fig 3.2. Concentrations of effluent Ca^{2+} , Mg^{2+} and SCN^-	36

Fig 3.3. Surface complexes distribution at 25°C.....	38
Fig 3.4. Surface complexes distribution at 130°C.....	38
Fig 3.5. Concentration ratio of surface complexes vs injected pore volume at 25°C.	39
Fig 3.6. Concentration ratio of surface complexes vs injected pore volume at 130°C. ..	40
Fig 3.7. Chemical analysis of Ca^{2+} at 25,60,130,150°C.....	40
Fig 3.8. Chemical analysis of Ca^{2+} at 25,60,130,150°C.....	41
Fig 3.9. Concentration ratio of surface complexes vs injected pore volume at 60°C.	41
Fig 3.10. Concentration ratio of surface complexes vs injected pore volume at 150°C. 42	
Fig 3.11. Concentration ratio of surface complexes vs injected pore volume at 60°C. ..	43
Fig 3.12. Concentration ratio of surface complexes vs injected pore volume at 150°C. 43	
Fig 3.13. concentration ratio of $>\text{CO}_3\text{Ca}^+$ vs injected pore volume	45
Fig 3.14. Concentration ratio of $>\text{CO}_3\text{Mg}^+$ vs injected pore volume.....	45
Fig 3.15. . Concentration ratio of $>\text{CaCO}_3^-$ vs injected pore volume.....	46

LIST OF TABLES

	Page
Table 1.1. Wettability and flow characteristics relation.	15
Table 1.2. Wettability expressed by contact angles	19
Table 2.1. Reactions for calcite and dolomite surface.....	32
Table 3.1. Composition of brine 1 and brine 2.	34
Table 3.2. Parameters used in Crunchflow.	34
Table 3.3. Surface sites concentration ratios at different temperatures.....	47
Table 3.4. Mineral fractions at different temperatures	48
Table 3.5. . Oil recovery percentage and calcite dissolution relation.....	49

NOMENCLATURE

Symbol	Description
k_1, k_2, k_3	Reaction rate constants for mineral dissolution (mol/m ² /s)
Δ_H	enthalpy change (J/mol)
K_{eq}	equilibrium constant
SSA	Specific surface area (m ² /g)
v	Flow velocity vector (m/s)
V_X	Velocities in longitudinal direction (m/s)
V_Y	Velocities in transverse direction (m/s)
α	Longitudinal dispersivity (cm)
LogK	Logarithm of K_{eq}
D	Combined dispersion-diffusion tensor (m ² /s)
R	Gas Constant
D^*	Effective diffusion coefficient in porous media (m ² /s)
C	Total concentration of ions (mol/m ³)
P_C	Capillary pressure
P_{nw}	Pressure of nonwetting phase
P_w	Pressure of wetting phase
σ_{ow}	Interfacial tension between oil and water
θ	Contact angle measured through the water

1 INTRODUCTION

Waterflooding is widely used technique in upstream oil industry for oil recovery. Extraction methods of oil are broadly classified as primary, secondary and tertiary oil recovery techniques. Primary oil recovery techniques are those which do not require injection of gas or liquid to enhance production. These techniques include use of natural energy to produce oil. Natural reservoir energy is available in the form of gas-cap, water drive, gravity drainage, solution gas drive and combination of these drives. The reservoir pressure available in initial stage of production, is usually higher than bottom hole pressure. This pressure difference drives hydrocarbon up to the surface. The reservoir pressure is maintained by above mentioned drives (water, gas, gravity). Hence, to continue oil production, it is necessary to keep this differential pressure maintained by either reducing bottom hole pressure or increasing reservoir pressure. This differential pressure is maintained by using artificial lift technique. The extraction potential is only 5 to 15% for primary techniques. Primary recovery stage reaches its limit when either reservoir pressure is so low that production rate declines significantly or water or gas production is significantly increased. When primary recovery techniques fail to stimulate production, secondary recovery techniques are used. These include injection of gas or water into reservoir through injection wells to increase pressure and stimulate production. Waterflooding is considered as secondary oil recovery method.

In waterflooding, water is injected into reservoir to support pressure necessary to produce oil. Since water is cheapest and readily available for waterflooding, it is one of the cheapest techniques used for oil recovery. For many years, waterflooding was technique considered to improve oil recovery by maintaining reservoir pressure. In recent years,

geochemical aspect of waterflooding was studied. Many researchers proposed new chemical mechanisms that takes place in reservoir when water (brine) with different composition compared to initial formation water composition. This injecting brine composition has profound effect on the wettability alteration.

1.1 OIL RECOVERY METHODS

Oil production starts after drilling and completion of well. Oil is produced in several stages. These stages are often referred as oil recovery techniques.

- Primary production: Primary and artificial lift
- Secondary oil recovery: (For maintaining pressure by means of waterflooding)
- Tertiary oil recovery: (Enhanced production by injecting gas, chemicals, polymers and surfactants).

Period of production is divided into stages based on amount of pressure available in the reservoir to produce oil. In early period of production, reservoir pressure is usually in abundance. Natural driving mechanism determines overall pressure energy available for production. When production starts, as high pressure energy is readily available, reservoir fluids flow to the surface through wellbore. As pressure starts declining, artificial lift can be used. Presence of aquifer can help maintain reservoir pressure naturally. It is known as water drive mechanism. The pressure loss during production is directly proportional to volume of hydrocarbon produced. Hence production rate drop indicates low reservoir pressure. When oil production rate drops down significantly after using artificial lift, secondary and tertiary oil recovery techniques are used. Fig 1.1 shows the production

phases in terms of pressure energy. These stages of production just give idea about overall production techniques and when they are used. It is not always profitable to produce oil with same sequence. Selection of recovery technique depends not only on reservoir pressure but also on factors like cost of recovery, current oil prices, availability of equipment and injecting material and recovery factor.

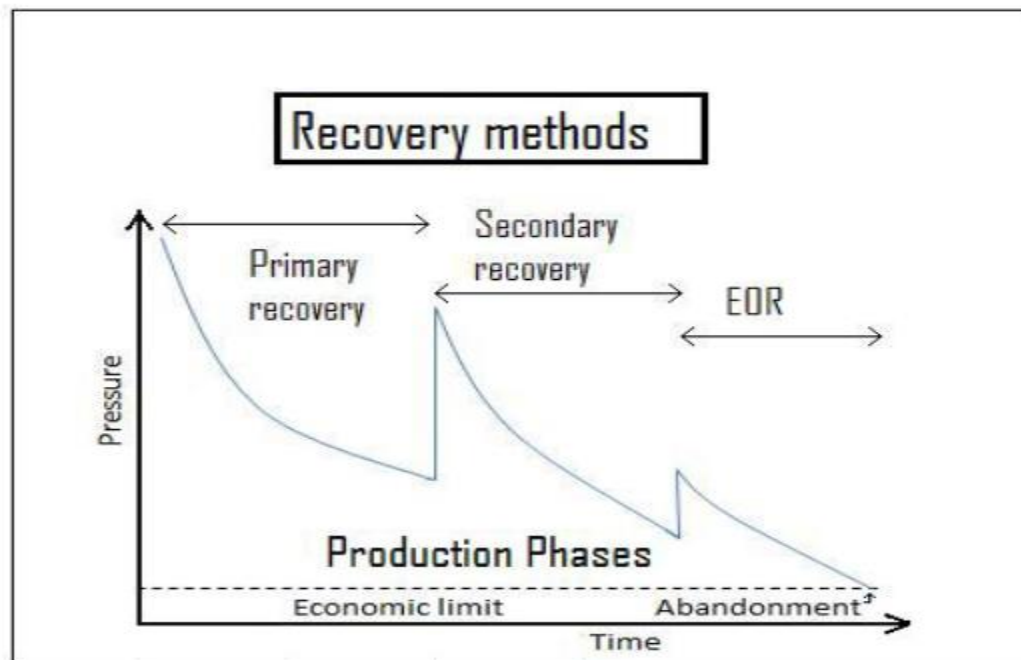


Fig 1.1. Production phases. (Based on Raymond and Leffler, 2006).

1.1.1 Primary Oil Recovery Methods. Primary oil recovery is method which utilizes natural pressure energy from the reservoir to produce hydrocarbon. The availability of natural pressure energy depends on existing natural drive mechanisms. Water drive, gas cap drive, solution gas drive, gravity drainage are the main natural drive mechanisms that assist oil production during initial production period. Water drive mechanism consists of presence of water aquifer which exerts large pressure into the reservoir. It also helps for maintaining reservoir pressure when oil is produced. Gas cap drive includes presence of

gas cap on top of hydrocarbon zone. As oil production starts, the gas from gas cap expands and maintains pressure. Water drive and gas cap drive help maintain pressure for many years of continuous production. In solution gas drive, gas is dissolved in the oil. As production starts, pressure drops, and this oil and gas mixture expands and provides necessary energy needed for production. The natural energy from solution gas drive is many times not long lasting and sufficient to produce oil.

Overall, primary oil recovery recovers oil in the range of 10% to 15% oil of original oil in place. Recovery from primary oil recovery depends on-

- Amount of original oil in place and its distribution in reservoir
- Fluid and rock properties
- Production rate and drive mechanism
- Economic factors

When fluids are not capable of flowing to the surface by the mean of natural energy, artificial gas lift methods and electric pumps are used to bring reservoir fluids to the surface.

1.1.2 Secondary Oil Recovery Methods. When oil production rate drops considerably after primary oil recovery production phase, organizations may decide to use secondary oil recovery methods. In secondary oil recovery methods, water or immiscible gases are forcefully injected into the reservoir using injecting wells. The main goal of this method is to maintain reservoir pressure to produce oil at desirable rate. Production rate depends on availability, oil prices and many other factors. Hence, use of this method depends on desirable production rate. Waterflooding is most common term used for

secondary oil recovery. Immiscible gas flooding is rarely used compared to waterflooding. Thus, secondary oil recovery includes-

- Waterflooding
- Immiscible gas flooding

To achieve maximum oil recovery through waterflooding or gas flooding, various factors such as lithology, reservoir geometry, permeability, porosity, fluid saturation, fluid properties, continuity of rock properties, reservoir depth, relative permeabilities, water source and its chemistry are taken into consideration. During early uses of waterflooding, chemical behavior of rock and injected water was not taken into consideration. But recently, it is found that this chemical behavior leads to wettability alteration. But, as primary purpose of secondary oil recovery methods is to boost natural energy, waterflooding as secondary oil recovery is still considered for maintaining reservoir pressure. Using secondary oil recovery methods, 15% to 20% oil can be recovered. A suitable candidate reservoir can produce total 40-50% oil using primary and secondary oil recovery methods.

1.1.3 Tertiary Oil Recovery Methods. Tertiary oil recovery methods are also known as enhanced oil recovery methods. These methods involve injection of chemicals, surfactants, polymers, miscible gases to produce oil by reducing viscosity of oil or increasing overall sweep efficiency. There are many definitions used by many organizations to describe tertiary oil recovery. For sake of simplicity, enhanced oil recovery is defined as “oil recovery by injection of materials not normally present in the reservoir” (Lake, 2010).

Chemically modified water injection can be considered as tertiary oil recovery method or enhanced oil recovery method since this water is not already present in the reservoir. It was also seen that when chemically modified water injected into the reservoir, it alters the wettability which can lead to improved oil recovery.

Main objectives of enhanced oil recovery are-

- Like secondary oil recovery, EOR can be used to maintain reservoir pressure at desired level
- Increase the displacement efficiency. Microscopic displacement efficiency indicates extents of oil flow at pore scale. Reducing residual oil saturation can increase displacement efficiency. Interactions between displacing fluid and oil determine microscopic displacement efficiency. These interactions can be chemical or physical such as change in IFT between the fluids, decrease in oil viscosity, oil volume expansion (Green and Willhite 1998).
- Improving sweep efficiency which depends on mobility ratios. Improving mobility ratio improves sweep efficiency. Sweep efficiency is measured in horizontal direction (areal sweep efficiency) and vertical direction (vertical sweep efficiency). It is degree to which flood have moved the displaced fluid
- fluid through the reservoir before reaching the producing well. (Green and Willhite 1998).

Sweep efficiency is related to macroscopic scale, and displacement efficiency is related to microscopic scale. Different EOR techniques emphasize on different types of displacements. For example, Alkaline flooding accounts for improved displacement efficiency by altering rock wettability. Polymer flooding affects sweep efficiency by

increasing water viscosity. (Bavière 1991). Fig 1.2 (Alvarado and Manrique) shows EOR methods used in several types of rocks.

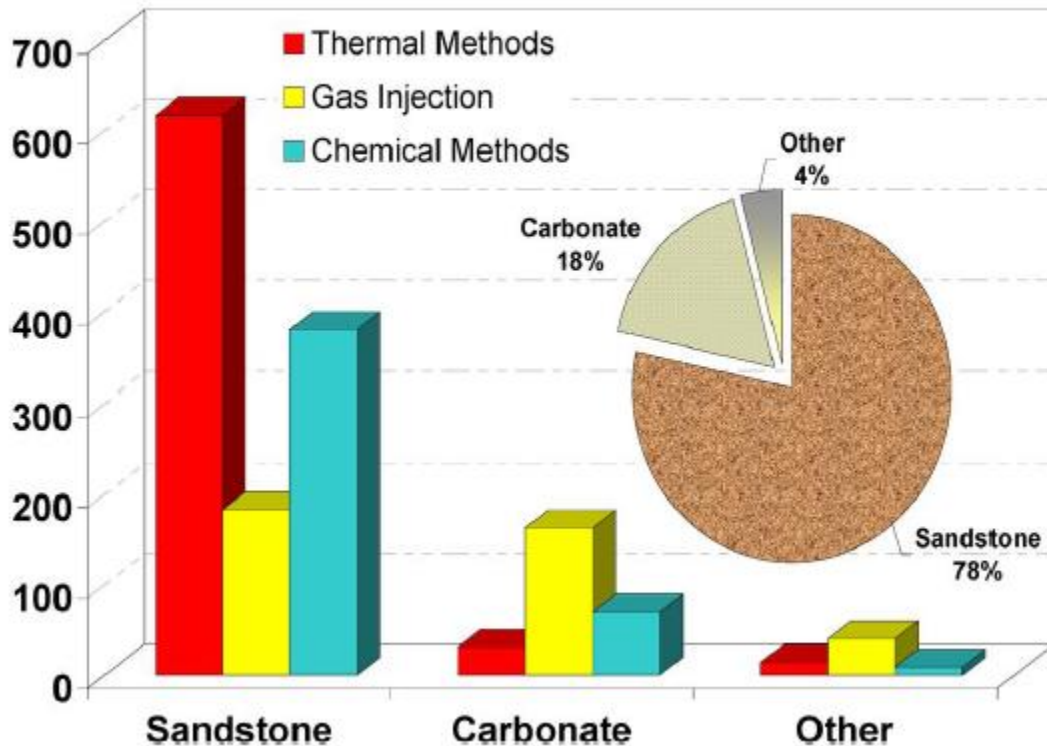


Fig 1.2. EOR methods by lithology. (Alvarado and Manrique, 2010).

In high/low salinity waterflooding, oil recovery is improved due to effect of improved microscopic displacement efficiency. High or low salinity water is immiscible fluid. Hence, forces related to displacement efficiency are capillary, viscous and gravity forces acting on fluid droplets. Capillary forces occur at the interface of wetting and non-wetting fluids. At microscopic scale, capillary forces are greater than any other forces such as viscous and gravity forces.

Capillary pressure is defined as pressure difference across the interface of two immiscible fluids. Imbibition and drainage processes have considerable influence on

capillary pressure (Thakur and Satter, 1998). Imbibition is process in which non-wetting fluid is displaced by wetting fluid, whereas, drainage is the process in which wetting fluid is displaced by non-wetting fluid. These two processes are either aided or opposed by capillary forces (Ahmed, 2006). Capillary forces in a reservoir are the result of the combined effect of interfacial and surface tension, pore geometry and size, and wetting characteristics of the system (Ahmed, 2006).

Mathematically, capillary pressure can be expressed as

$$P_c = P_{nw} - P_w$$

where,

P_c = Capillary pressure

P_{nw} = Pressure of nonwetting phase

P_w = Pressure of wetting phase

Considering oil as non-wetting phase, and water as wetting phase, the formula can be written as

$$P_c = P_o - P_w = \sigma_{ow}C = \frac{2\sigma_{ow}\cos\theta}{r}$$

where,

σ_{ow} = Interfacial tension between oil and water

C = Mean curvature of the interfacial tension

r = Radius of cylindrical pore channel

θ = Contact angle measured through the water

Capillary forces, surface tension, interfacial tension and wettability are important properties in microscopic scale. Hence, high salinity waterflooding can be considered as

EOR related to microscopic displacement efficiency. Also, it can be placed as chemical or miscible class of EOR.

1.2 BRINE COMPOSITION AND WATERFLOODING EFFICIENCY

For many years, waterflooding was used as secondary recovery technique which maintains or increases reservoir pressure to increase oil production. In recent years, lot of research is focused on geochemical reactions and chemical mechanism that takes place between rock-oil- water system. Many laboratory studies proposed that crude oil, rock and brine tend to form chemical equilibrium. During the process of achieving chemical equilibrium, wettability is altered. This wettability alteration leads to increase or decrease oil recovery. Hence, ultimately, we can say that waterflooding efficiency is function of wettability alteration and so brine composition.

Composition of rocks and minerals are also equally important to understand geochemical trend and chemical behavior of rock-oil-brine system. Carbonates and Sandstone rocks have different chemical compositions. Interaction of different types of rocks with different brine composition leads to varying chemical behavior. It is very important to understand this varying chemical behavior to achieve optimum oil recovery by waterflooding technique.

Studies found that seawater depleted in NaCl led to increased oil recovery (Fathi, et al., 2011). Seawater brine contains Ca^{2+} , Mg^{2+} , SO_4^{2-} as potential determining ions which change the surface charge of carbonate rock and lead to wettability alteration (Zhang et al., 2006).

Coreflooding studies in laboratories proved this fact. Fig 1.3 shows oil recovery percentage for different brine compositions containing different concentrations of SO_4^{2-} ions for chalk cores at 100°C . In this case, increasing concentration of SO_4^{2-} in injecting brine led to increased oil recovery at same temperature.

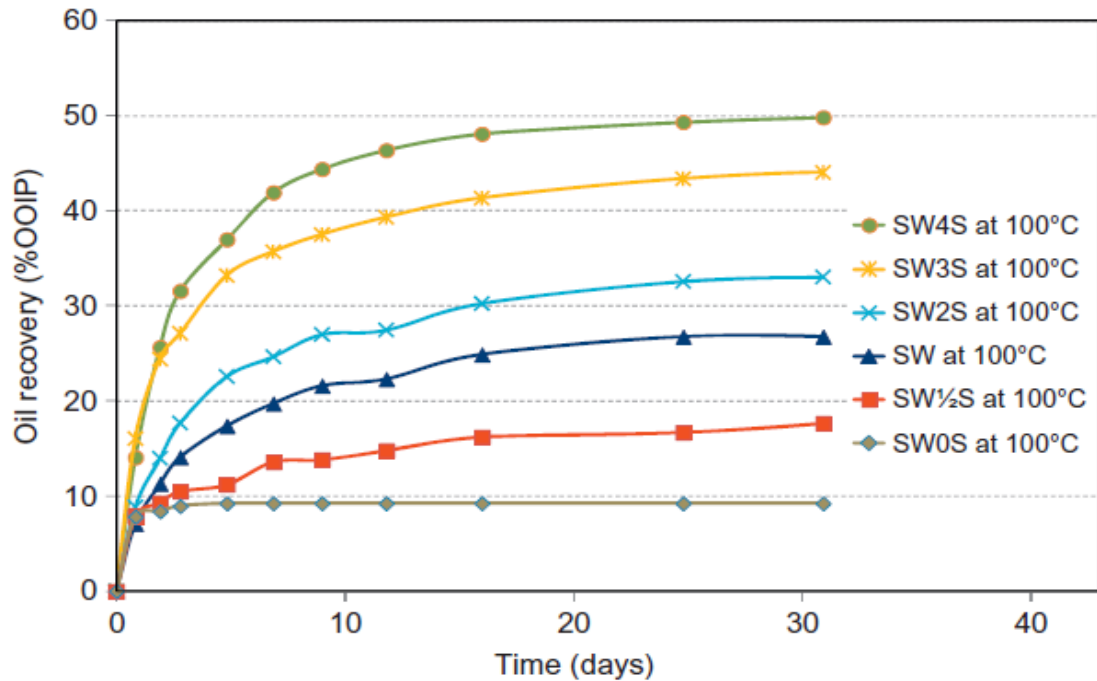


Fig 1.3. Oil recovery by spontaneous imbibition. Sulfate-modified SW was used into chalk cores at 100°C . (Zhang and Austad, 2006).

Fig 1.4 shows effect of modified seawater with increasing calcite concentration at 70°C on oil recovery. It can be seen here that oil recovery improved for same temperature, when Ca^{++} concentration in injection brine was increased. Finally, when it was increased to 4 times, oil recovery reached to 68% approximately. This increase in oil recovery is due to Ca^{++} ion to bonding of calcite ion with oil carboxylic group which is negatively charged.

Studies found that low salinity waterflooding improves oil recovery in sandstone reservoir. However, for carbonate reservoirs, high salinity water is used to improve oil

recovery. Recent studies showed that low salinity waterflooding improved oil recovery by 4% of OOIP (original oil in place).

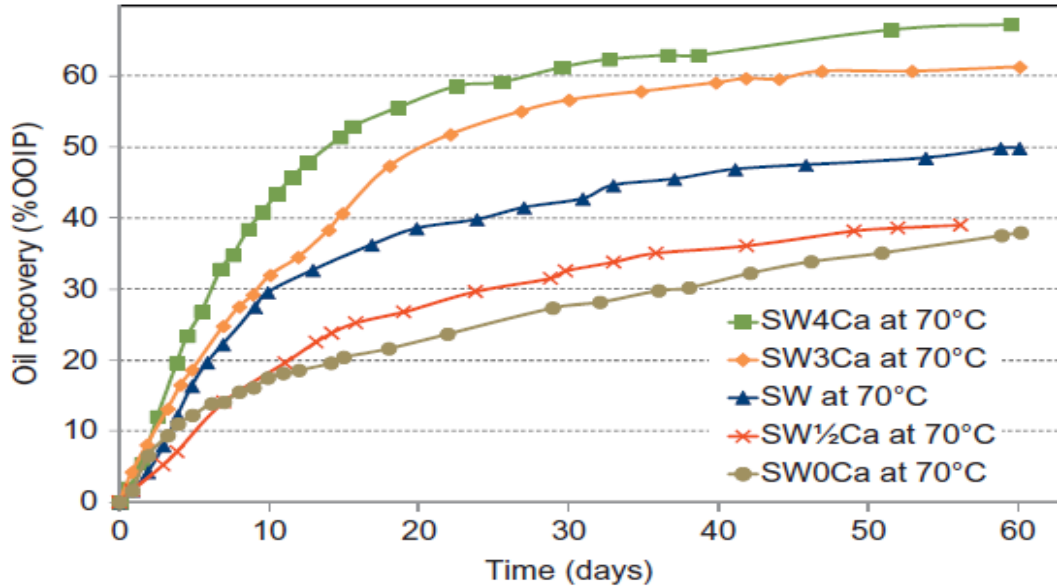


Fig 1.4. Oil recovery by spontaneous imbibition. Calcite-modified SW was used into chalk cores at 70°C. (Zhang and Austad, 2006).

All experimental study was conducted using coreflooding techniques. Coreflooding technique is used in laboratories to emulate actual reservoir conditions and oil recovery method from field. At first, field conditions are studied. Necessary data is gathered to emulate these conditions in labs. Generally, rock samples from same reservoir are cut into cylindrical shape and used as cores for coreflooding experiments. But, synthetically modified cores are also used for coreflooding. If cores are prepared from same rock samples, it is necessary to clean those cores to remove the sulfate and salts, which could affect the wetting properties. To remove these salts, cores are flooded with distilled water. Toluene is also used for cleaning cores at high temperatures.

Coreflooding setup is shown in Fig 1.5. The main setup consists of coreholder, transfer cells, pressure regulators and pump. Constant pressure is required to displace fluid throughout the coreflooding process. This constant pressure is provided by syringe pump. During experiment, core is kept in coreholder. This coreholder can be kept in oven if high temperature is required. Various accumulators are used to store brines and oil which are injected into the core as per requirement. Back pressure is required at output junction to keep outlet flow constant. Hence, back pressure regulator is also required. Differential pressure transducer is used to measure pressure difference between input and output pressures.

Coreflooding experiments for chalks (Fathi et al., 2011) showed that oil recovery factor increased from 38% to 45% when imbibing fluid was changed from seawater to seawater depleted in NaCl at 70°C. Also, recovery factor increased to 50% when sulfate concentration in seawater depleted in NaCl was increased to four times compared to sulfate concentration in initial formation water.

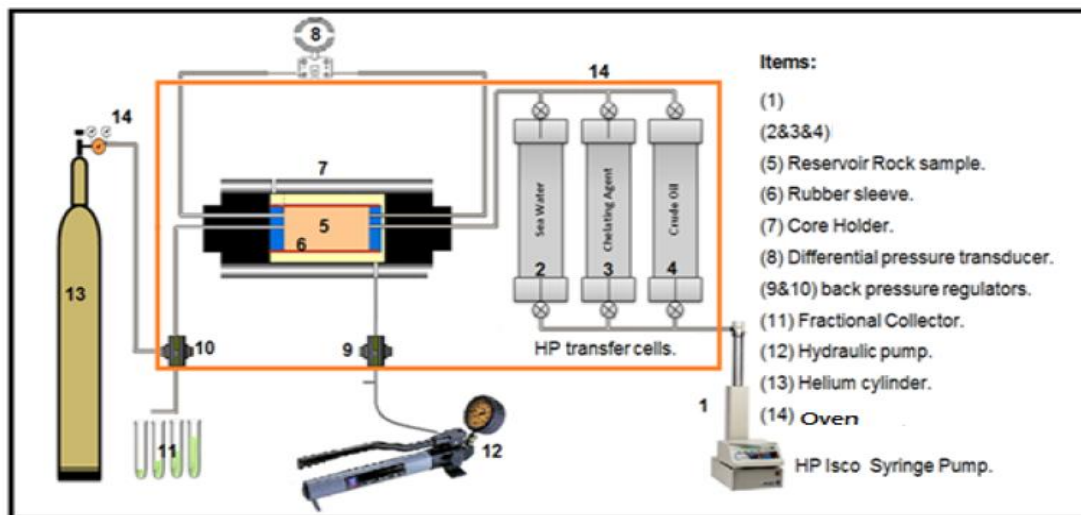


Fig 1.5. Flooding system.

1.3 WETTABILITY

Distribution of fluids in porous media is not only affected by forces at immiscible fluid interface such as capillary forces, gravity and viscous forces but also forces present at liquid-solid interface. Wettability is important property which describes interaction of solid and liquid. It is property of solid, particularly rock in reservoir engineering aspect. It is tendency of fluid to spread on or adhere to a solid surface in the presence of the other immiscible fluids (Ahmed, 2006). It is considered as property of rock because different rocks prefer different wetting fluids. Wettability has influence on capillary pressure, relative permeabilities and fluid saturation. Hence, fluid entrapment, distribution and flow in pore space are strongly affected by wettability (Thakur and Satter, 1998).

When two immiscible fluids are flowing in the reservoir, the fluid which makes rock surface wet is known as wetting phase, while another phase is known as non-wetting phase. Relative permeability is concept used in reservoir engineering if two or more fluids are flowing in the reservoir. It is defined as ratio of effective permeability of fluid to the absolute permeability. Effective permeability is property of fluids, and is measured in laboratories using rock cores, while absolute permeability is property of porous media and it is capacity of the porous medium to allow fluid flow. Thus, relative permeability can be expressed as-

$$k_{rf} = \frac{k_f}{k}$$

Where k_{rf} = Relative permeability of fluid (oil, water or gas)

k_f = Effective permeability of fluid (oil, water or gas)

k = Absolute permeability of fluid (oil, water or gas)

Relative permeability curves are strongly affected by wettability. Relative permeability curve is shown below in Fig 1.6. The curve presents oil-water system with water as wetting phase, and oil as non-wetting phase. It shows effect of changing wettability on relative permeabilities of oil and water.

In this study wettability was altered by changing concentration of additives in oil and water. θ indicates contact angle which is measurement for wettability. Dark thick lines are indicating relative permeability curves for water, while, thin lines are indicating relative permeability curves for oil. Fig shows that intersection of relative permeability curves of water and oil shifts to right and maximum k_{rw} decreases with increase in water wetting. Many other researchers (Morrow et al., 1973, McCaffery and Bennion et al., 1974, Trieber et al., 1972) also studied effects of wettability on relative permeabilities and saturations of oil and water. Table 1 below shows the relation of flow characteristics and wettability (Bavière, 1991).

Wettability depends on chemical composition of oil, water and composition of rocks. Hence, rocks can be either oil-wet or water-wet depending on chemical and physical compositions of oil, water and rock. To classify rock as water-wet or oil-wet, it is necessary to measure the wettability. Wettability is measured in terms of contact angle (θ). This contact angle varies from 0° to 180° . In hydrocarbon reservoir, two phases such as gas and liquid, two immiscible liquids, solids and liquids are separated by interface between them. Interfacial tension is related to adhesion tension. This tension determines which fluid will wet the solid (rock surface).

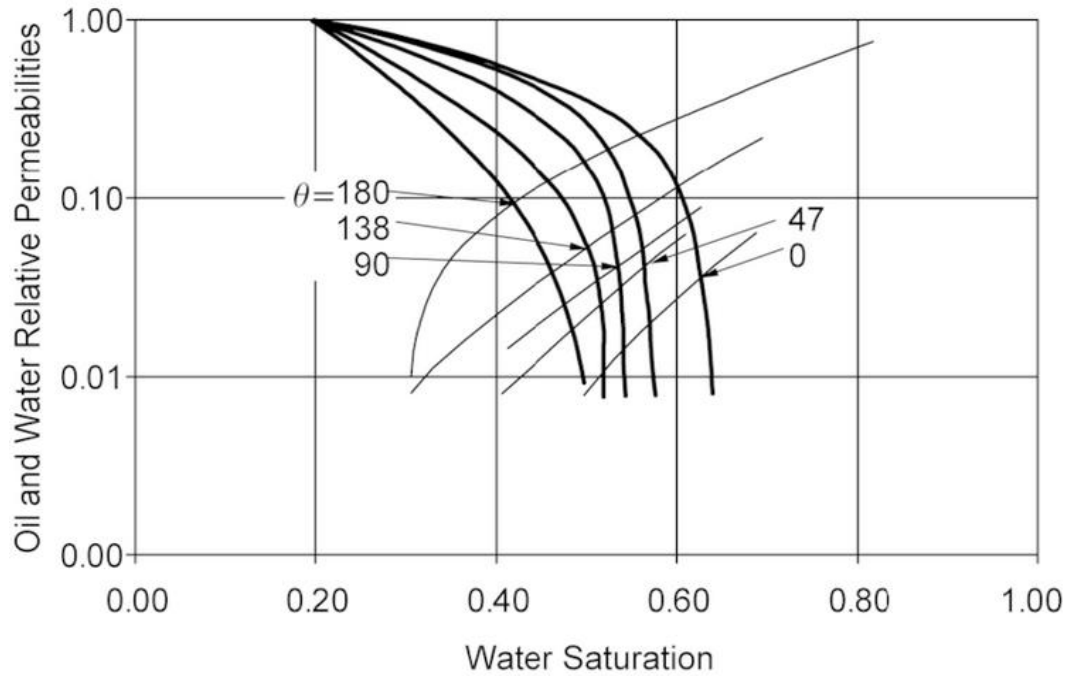


Fig 1.6. Effect of rock wettability on oil-water relative permeabilities. (Owens and Archer, 1971).

Table 1.1. Wettability and flow characteristics relation. (Bavière, 1991).

	Water-Wet	Oil-Wet
Connate water saturation	Usually greater than 20 to 25% pore volume	Generally less than 15% pore volume, frequently less than 10%
Saturation at which oil and water relative permeabilities are equal	Greater than 50% water saturation	Less than 50% water saturation
Relative permeability to water at maximum water saturation; i.e., floodout	Generally less than 30%	Greater than 50% and approaching 100%

Adhesion tension is given by following equation.

$$AT = \sigma_{so} - \sigma_{sw} = \sigma_{wo} \cos \theta$$

Where,

σ_{so} = Interfacial tension between solid and lighter liquid

σ_{sw} = Interfacial tension between solid and denser liquid

σ_{wo} = Interfacial tension between lighter liquid and denser liquid

When rock prefers one fluid to adhere over other fluid, different type of overall wettability is established in the system (Thakur and Satter, 1998). Since, capillary pressure and relative permeability, which are crucial factors for oil recovery, are affected by wettability, it also controls ultimate oil recovery. Fig 1.9 shows dependence of oil saturation on wettability.

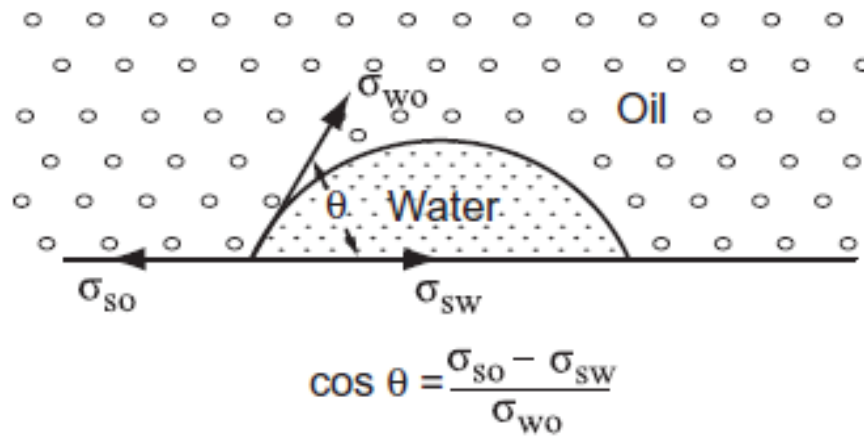


Fig 1.7. The interfacial tension values and contact angle.

Reservoir rocks are generally classified based on wettability as water-wet and oil-wet rocks. Fig 1.8 shows water-wet and oil-wet rocks.

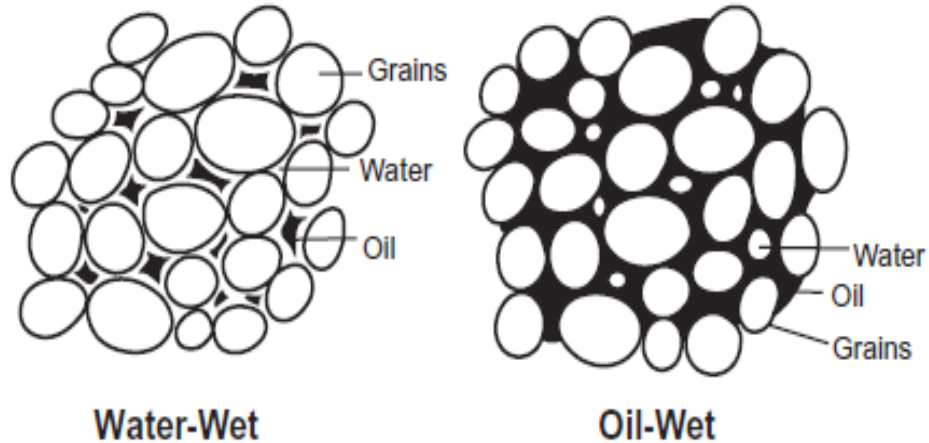


Fig 1.8. Idealized representation of water-wet and oil-wet reservoir rocks.

Wetting phase usually prefers to stick to smaller pores having small openings. Thus, if system is water-wet then waterflooding causes water to enter into small pores with small openings. This water squeezes oil to larger pores. In larger pores with large pore openings, oil can easily flow. Preferential wetting of rock surface helps water phase to maintain fairly uniform front with the oil displaced in front of it. Sometimes, this flowing oil fails to connect with remaining oil in the pores and breaks off which leads to oil drops trapped into the pores at center surrounded water and rock. This is known as residual oil saturation. This trapped oil is immobile, and no additional oil is recovered after water breakthrough in strongly water-wet system (Agbalaka, Dandekar et al., 2008). The oil droplet trapped into the pore center surrounded by rock and water is shown as water-wet system in Fig 1.5.

In strongly oil wet reservoir, waterflooding results in formation of water channels or fingers through the center of larger pores squeezing oil to smaller pores. Oil sticks to the rock surface in small pores and crevices as continuous film over pore space, pore throat (Agbalaka, Dandekar et al., 2008).

Mixed wettability can also occur in reservoir due to heterogeneity or variation in mineralogy of exposed rock surface or cementing material surfaces (Green and Willhite 1998). Reservoir rock wettability is strongly affected not only by rock mineralogy and composition but also adsorption and desorption of components in oil phase, rock surface and film deposition. Mixed wettability is range of water-wet to oil-wet system. Some reservoirs have heterogeneous wettability with variation in wettability preferences on different surfaces (Anderson, 1987). Contact angel method, Amott wettability test are methods to measure wettability. Already described, contact angle measurement is most conventional method for determining wettability.

When oil and water come in contact with solid, if the measured contact angle is 90° , wettability is expressed as neutral wettability. This indicates that both fluids tend to wet the surface. When contact angle close to is 180° , the system is considered as strongly oil wet system. The ranges of contact angles and wettability preferences are shown in table 1.2 (Rezaeidoust, 2011).

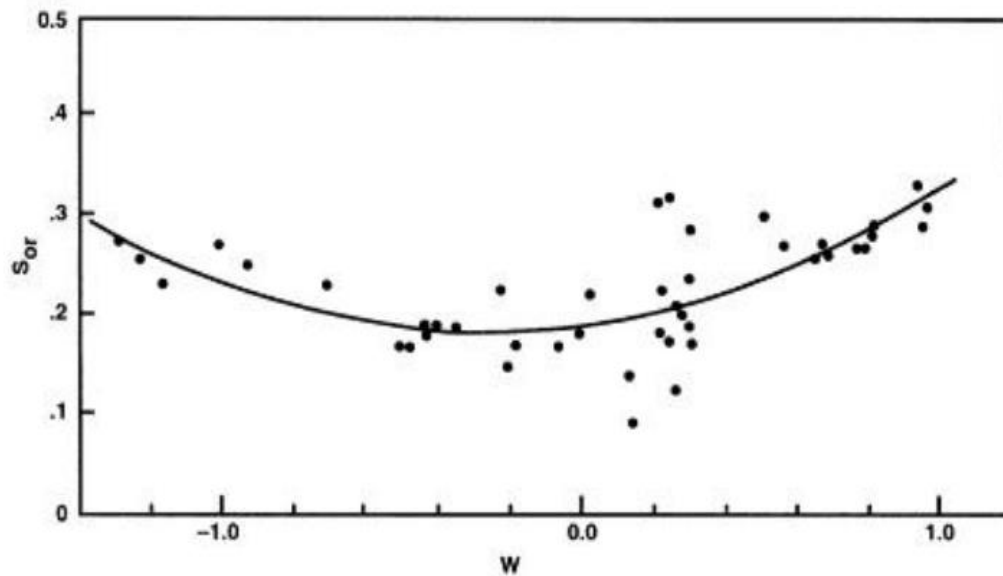


Fig 1.9. Dependence of oil saturation on wettability. (Thakur and Satter, 1998).

The main drawback of contact angle measurement method is that the experimental value of contact angle depends on image magnification. Direct goniometer is used to measure contact angle.

Table 1.2. Wettability expressed by contact angles. (Rezaeidoust, 2011)

Contact angle values	Wettability preferences
0-30°	Strongly water-wet
30°-90°	Preferentially water-wet
90°	Neutral wettability
90°-150°	Preferentially oil-wet
150°-180°	Strongly oil-wet

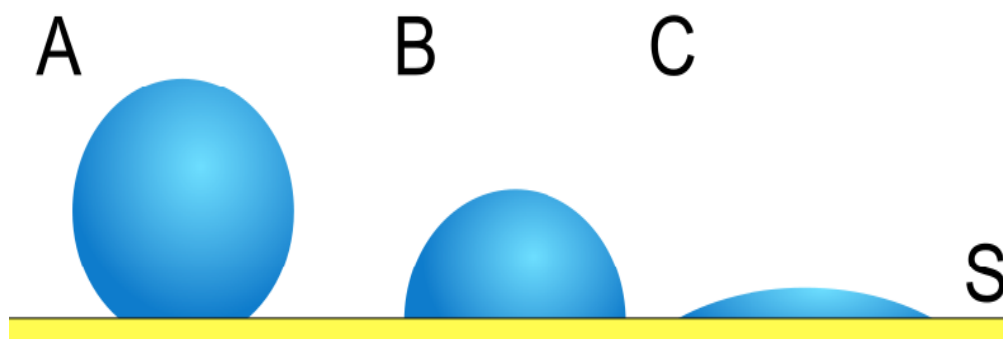


Fig 1.10. Wetting conditions on solid. (A: Non-wetting phase, B: Intermediate wetting phase, C: Wetting phase).

For small contact angles below 20°, acquiring accurate measurements is very difficult. This is due to uncertainty in drawing tangent line when the droplet profile is

almost flat (Yuan and Lee, 2013). Also, geometric form of solid sample can affect contact angle measurement.

Amott wettability test is another method used for determining wettability. It is based on capillary pressure phenomena and determination of Amott wettability index. If wettability index is 1.0, it indicates strongly wetting index whereas, index of 0.0 indicates strongly non-wetting index (Thakur and Satter, 1998). This method neglects capillary pressure curve hysteresis, and thus, can be misleading if system is fractionally wet (McDougall and Sorbie 1995).

Generally, sandstone and carbonate reservoirs are water-wet before contact with crude oil, but may change to oil-wet by components of crude oil. Certain minerals may be variably prone to water or oil-wet. Also, any treatment that can change the wettability of the formation from water-wet to oil-wet can significantly impair productivity.

Other techniques used for wettability measurements include imbibition rate test, hysteresis of relative permeability curve, United States Bureau of Mines (USBM) wettability test and Nuclear Magnetic Relaxation (Agbalaka, Dandekar et al. 2008).

1.4 FACTORS AFFECTING WETTABILITY OF ROCK

Several factors affect wettability of rock including oil composition, pH, brine composition, ionic strength, mineral surface, pressure, temperature and traces of multivalent cations (Anderson, 1986).

Oil and Brine Composition Interaction- Crude oil contains organic matter including asphaltene and resin, which are rich in polar compounds of acidic and basic nature. This

composition of crude oil is very important parameter for wettability alteration. It affects wettability in two ways.

1. Polar components exhibit surface activity
2. Oil creates solvent environment

Four wettability alteration mechanisms by crude oil were identified as follows:

- Polar interaction between oil and solid in the absence of water
- Precipitation on surface, depending upon behavior of oil as solvent
- Acid/base interactions between the opposite charged interfaces
- Specific interaction charged sites and multivalent ions

Surface charge of rock surface and fluid interface is strongly affected by important factors such as brine composition, pH and salinity which ultimately results in wettability alteration.

Oil recovery in carbonate reservoirs is generally less than 30% due to low water wetness, natural fractures, low permeability and heterogeneous rock properties. Carbonate rocks are chemically unstable rocks. At higher temperatures, many mineralization reactions take place in carbonate reservoir which may affect wettability. Carbonate surface is initially positively charged. When it comes in contact with crude oil, negatively charged carboxylic group ($-\text{COO}$) from crude oil gets bonded with positively charged carbonate surface. This carboxylic group ($-\text{COO}$) is important parameter responsible for wettability alteration in carbonate reservoir. The carboxylic group is determined by acid number, AN (mg KOH/g). The effect of this Acidic number, AN was studied by (Standnes and Austad, 2000a). It was found that the spontaneous imbibition rate and oil recovery decreased with increase in AN.

Fig 1.12 shows oil recovery with respect to time for different AN of carboxylic group used in diverse types of crude oils for spontaneous imbibition.

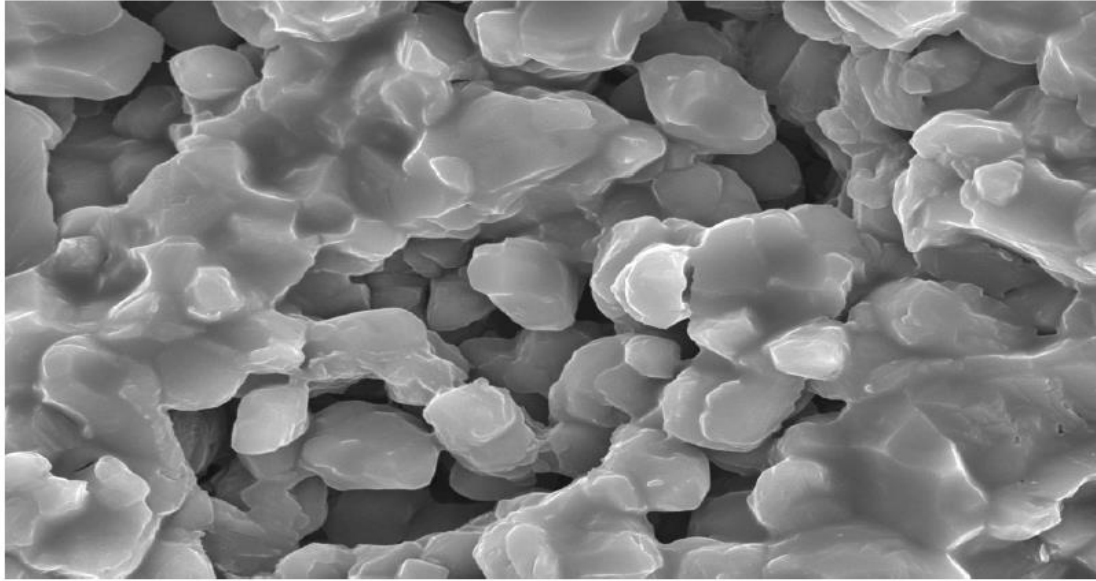


Fig 1.11. SEM image of carbonate section.

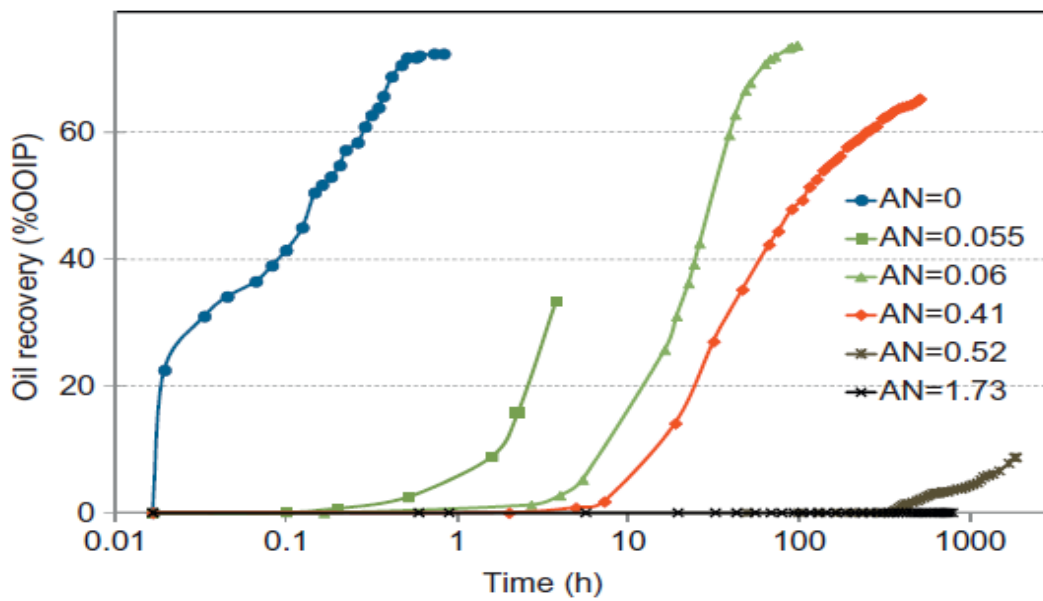


Fig 1.12. Spontaneous imbibition into chalk cores saturated with different oils. (Stadnes and Austad, 2000a).

AN of carboxylic group decreases as the temperature increases. Hence, at elevated temperature, carbonate reservoirs are more water-wet compared to low temperature reservoirs. At high temperature, decarboxylation of acidic material takes place. This process is catalyzed by solid CaCO_3 . Thus, initially, carbonate reservoirs are water-wet. When rock surface comes in contact with crude oil, it becomes oil-wet. The carboxylic group determined by AN is responsible for altering water-wet rock to oil-wet.

Spontaneous imbibition is the process in which wetting fluid displaces non-wetting fluid. Thus, water-wet rock contains water as wetting fluid and oil as non-wetting fluid. Hence, water as wetting fluid displaces oil (non-wetting fluid) which leads to improved oil recovery. Therefore, it is easier to produce oil from water-wet rock compared to oil wet rock.

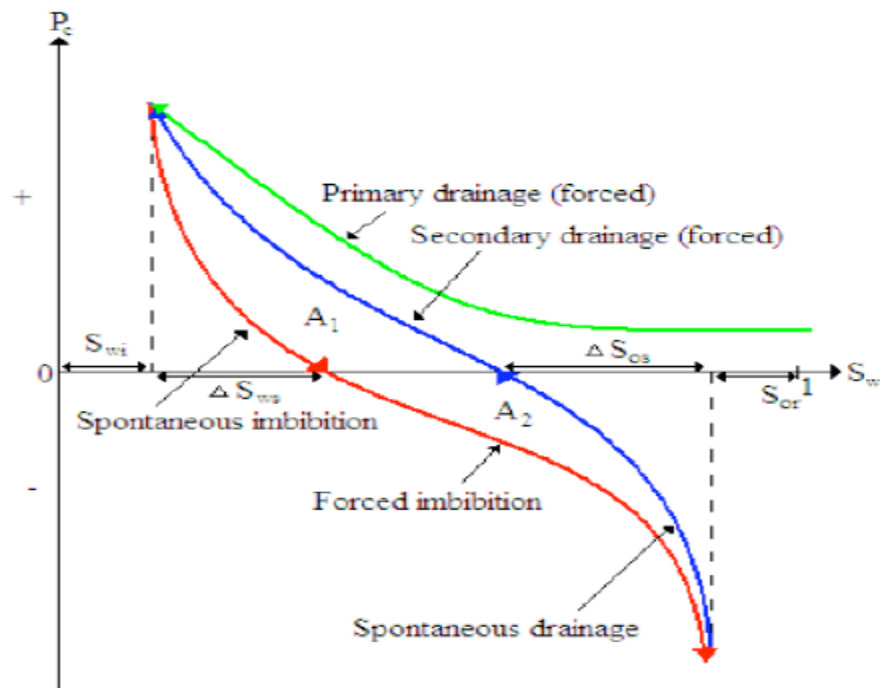


Fig 1.13. Capillary pressure diagram used to characterize wettability.

In recent studies, it was found that salinity of injected water and its composition can alter the wettability of reservoir. Usually, sea water is cheap and readily available source of injecting water used for waterflooding. Seawater contains ions like Ca^{2+} , Mg^{2+} and SO_4^{2-} which are reactive towards carbonate rock surface. These ions can act as potential determining ions and can change the surface charge of the rock (Pierre et al., 1990; Zhang and Austad, 2006). The affinity of these potentially determining ions was studied using chromatographic wettability test (Zhang et al., 2006; Zhang et al., 2007) and mechanism for wettability alteration was suggested.

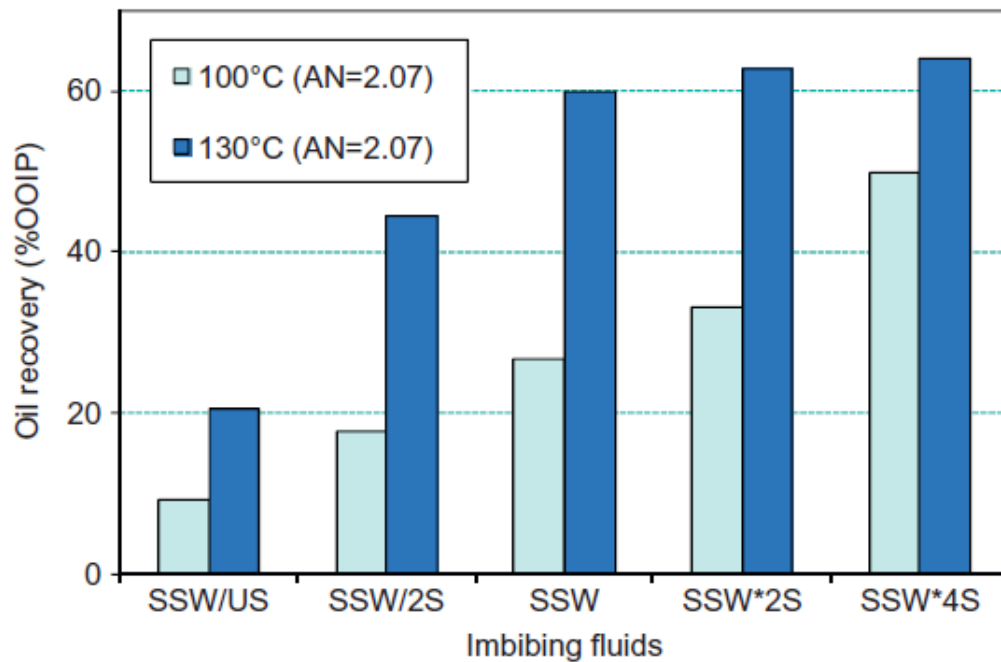


Fig 1.14. Maximum oil recovery from chalk cores at 100 and 130°C.

Desorption of carboxylic group from rock surface is first step of wettability alteration. As the SO_4^{2-} concentration in injecting water increased, affinity of SO_4^{2-} towards rock surface increases and it adsorbs on surface (Strand et al., 2006). This

adsorption of sulfate ions on rock surface removes carboxylic group attached to surface. Negatively charged carboxylic group couples with positively charged calcite (Ca^{2+}) ions. It is important to note that adsorption of sulfate onto the chalk promotes increasing co-adsorption of Ca^{2+} , which increases the concentration of Ca^{2+} at the surface to facilitate the reaction with adsorbed carboxylic components (Strand et al., 2006). Fig 1.15 shows the overall chemical mechanism for wettability alteration. At low temperatures such as 25°C , Mg^{2+} adsorbs less strongly than Ca^{2+} . At higher temperatures (130°C), Mg^{2+} substitutes Ca^{2+} , and degree of substitution increases with increasing temperature (Zhang et al., 2007).

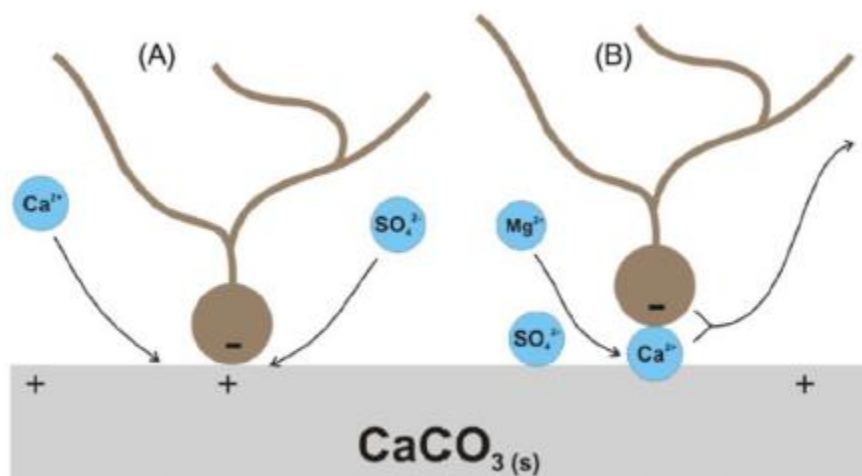


Fig 1.15. Suggested chemical mechanism for wettability alteration. (Zhang et al., 2007).

The impact of each of these potential determining ions on oil recovery was tested separately. As discussed earlier, oil recovery increased from 10% to 50% of original oil in place, as the concentration of SO_4^{2-} was increased from 0 to 4 times the concentration in ordinary SW. It is shown in Fig 1.3. Similarly, as the concentration of Ca^{2+} increased from 0 to 4 times the concentration in SW, oil recovery increased from 28% to 60%. Fig 1.4 shows increase in oil recovery with increase in Ca^{2+} concentration at 70°C . The reactivity

of Mg^{2+} towards rock surface increases as the temperature increases. Coreflooding study was conducted at 25, 130°C to understand the effect of Ca^{2+} and Mg^{2+} (Zhang et al., 2007). The concentration Ca^{2+} from effluent was increased at 130°C compared to that of 25°C. Concentrations of tracer (SCN^-) Ca^{2+} and Mg^{2+} are plotted for both temperatures. Plots are shown below in Fig 1.7. and Fig 1.8. Area between tracer curve and Ca^{2+} and Mg^{2+} gives quantitative measurement of adsorption. For 25°C, the area between tracer curve and Ca^{2+} is 0.290, and area between tracer curve and Mg^{2+} is 0.085 (Fig 1.7). This showed that the affinity of Ca^{2+} towards carbonate surface is 3.4 times stronger than that of Mg^{2+} . But, at 130°C, concentration of Ca^{2+} in effluent was significantly higher than the initial concentration (Fig 1.8).

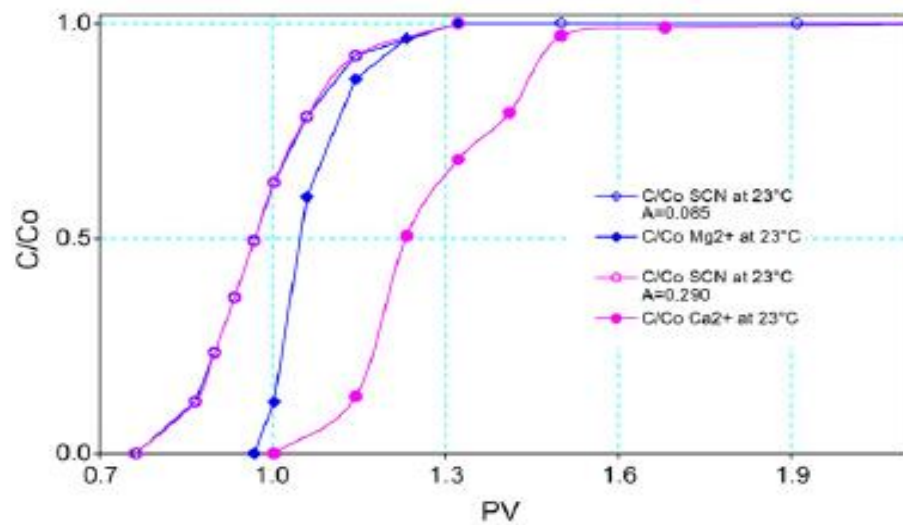


Fig 1.16. Competitive adsorption of Ca^{2+} and Mg^{2+} at room temperature. (Zhang et al., 2007).

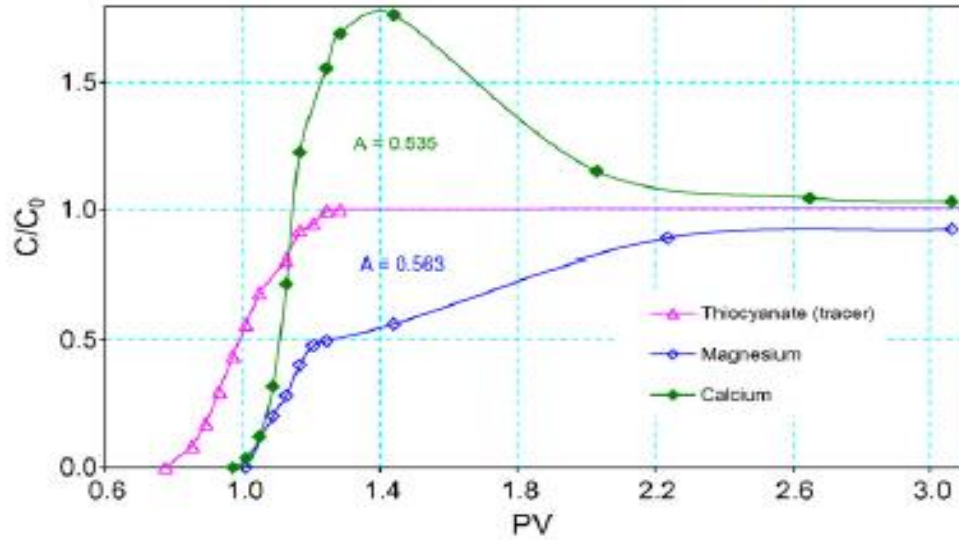


Fig 1.17. Competitive adsorption of Ca^{2+} and Mg^{2+} at 130°C . (Zhang et al., 2007).

1.5 OBJECTIVE

There are various reactions that occur on the surface of rock when it comes into contact with high salinity water. It is not possible to study these complicated reactions and processes using laboratory coreflooding experiments. Hence, it was important part of study to create reactive transport model which simulate environment similar to actual coreflooding environment and rock properties. By creating this reactive transport model, we modeled flow of high salinity brine through calcite rock. To model exact environment and chemical behavior of the system, various reactions, such as surface complexation reactions and mineral dissolution reactions that occur on the rock surface were taken into consideration. The reaction network is mentioned in methodology with equilibrium constants and rate values. These reactions with kinetics and thermodynamic data can help to understand chemical behavior of water-rock system. This behavior can be related to improved oil recovery which has oil-water-rock interaction that leads to wettability alteration.

2 METHODOLOGY

2.1 REACTIVE TRANSPORT

Crunchflow is the program used for simulating the water-rock interaction that takes place when seawater is flooded into the chalk core. Crunchflow code is written in FORTRAN 90, and it can be used for simulating many important processes, including reactive contaminant transport, chemical weathering, carbon sequestration, biogeochemical cycling, and water-rock interaction. It is based on finite volume discretization of the governing partial differential equations that can link flow, solute transport, multicomponent equilibrium and kinetic reactions in porous media. The governing mass conservation equation used by Crunchflow for reactive transport modeling is given below.

$$-\frac{d(c)}{dt} = \nabla(-D\nabla C + vC) + R_{CaCO_3} \quad (2.1)$$

Where, C is the total concentration of ions (mol/m^3). t is time (s); D is the combined dispersion-diffusion tensor (m^2/s); v is the flow velocity vector (m/s). D (dispersion-diffusion tensor) is sum of mechanical diffusion coefficient and effective diffusion coefficient.

In grid block, at any location, flow velocities in longitudinal and vertical direction are denoted by v_x and v_y . Their corresponding dispersion coefficients D_L and D_T are given by,

$$D = D^* + \alpha v \quad (2.2)$$

where D^* is effective diffusion coefficient. In this work, the value for effective diffusion coefficient was $1.7 \times 10^2 \text{ m}^2/\text{s}$. α is longitudinal dispersivity. The value used for this work

is 0.026 cm. In this work, spatial variation was not considered. Hence, effective diffusion coefficient and dispersivity values are kept same for each grid. There are total 25 grids in X direction, and 70 grids in Y direction. Each grid has size of 0.1 cm X 0.1cm.

Crunchflow code uses initial condition, chemical composition of rock, mineral type. Aging brine and condition was used as initial condition, and chemical composition of rock includes aging brine composition and rock composition. Calcite and small amount of dolomite was considered with porosity of 43%.

For time steps, 10 time intervals were considered from 0.01, 0.1, 0.2, 0.5, 1.0, 1.5, 2.0, 3.0, 4.0, 5.0, 6.0, 10 in hours. For breakthrough curves, these time steps were converted into pore volume (PV) using velocity and volume of block.

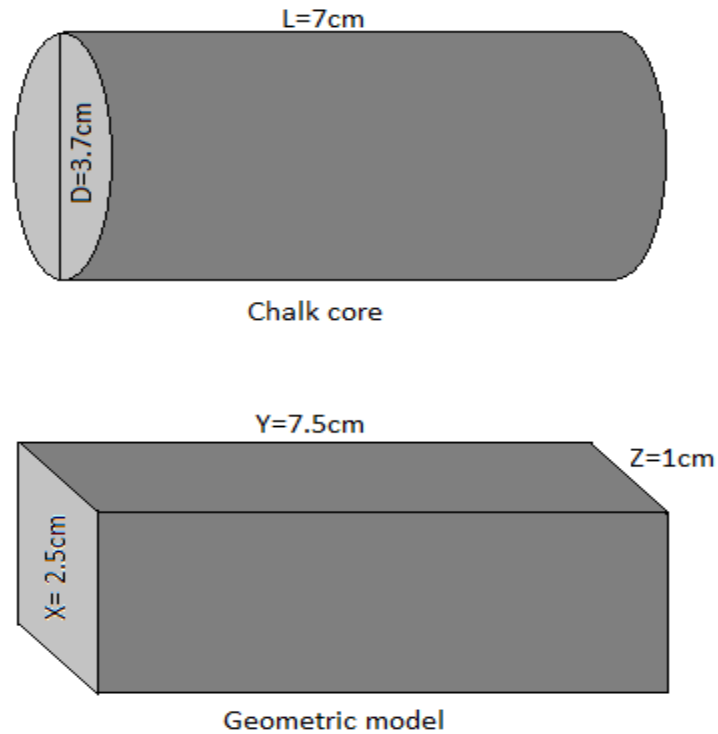
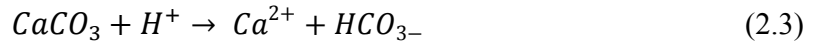


Fig 2.1. Dimensions of chalk core.

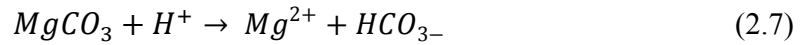
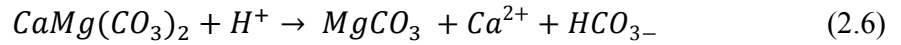
2.2 REACTIONS

To model the reactive transport process, mineral dissolution and precipitation is important step that needs to be considered. In this work, calcite and dolomite are minerals present on the chalk surface. Calcite and dolomite dissolution and precipitation are taken into consideration for the model. Reactions are taken from previous literature (Chou et al., 1989).

The dissolution reactions for calcite are shown below,



Small amount of dolomite is also present on the chalk core surface. The dissolution reactions for dolomite are shown below (Chou et al., 1989),



The reactions from (2.3) to (2.5) and (2.6) to (2.8) are elementary steps in dissolution process of calcite and dolomite respectively. The forward and backward rates for these reactions are expressed based on stoichiometry of three reaction steps and thermodynamic constraints. They are shown below (Chou et al., 1989),

For forward reaction,

$$R_f = k_1 a_H + k_2 a_{H_2CO_3^*} + k_3$$

$$R_b = k_{-1} a_{M^{2+}} a_{HCO_3^-} + k_{-2} a_{M^{2+}} a_{HCO_3^{2-}} + k_{-3} a_{M^{2+}} a_{CO_3^{2-}}$$

k_1, k_2, k_3, k_{-3} are rate constants (mol/m²/s). The values of k_1, k_2, k_3, k_{-3} were determined experimentally (Chou et al., 1989). Their values are 8.5×10^{-1} , 5×10^{-4} , 6.5×10^{-7} (mol/m²/s) for k_1, k_2, k_3 respectively. Similarly, for dolomite, 2.6×10^{-3} , 1.0×10^{-4} , 2.2×10^{-8} (mol/m²/s) are values for k_1, k_2, k_3 respectively. For reactive transport process modeling in Crunchflow, various components in the database are divided into primary and secondary species. Primary species are main building blocks for particular problem. Secondary species are those for which equilibrium reaction relationship is assumed with primary species in the problem. In this reactive transport model, primary species are H^+ , Cl^- , HCO_3^- , Mg^{++} , Ca^{++} , Na^{++} , K^+ , SO_4^- , SCN^- . Secondary species include OH^- , $CO_2(aq)$, HSO_4^- , CO_3^{--} , $MgSO_4(aq)$, $CaSO_4(aq)$. Also, there are active surface sites on the rock surface, which play important role in wettability alteration. These surface species are $>CaOH^{2+}$, $>CaOH$, CO_3^- , $>CaSO_4^-$, $>CO_3Mg^+$, $>CO_3H$, $>CaO^-$, $>CaCO_3$, $>CaHCO_3^-$, $>MgOH$, $>CaHCO_3^-$, $>CO_3Ca^+$, $>CaOH^{2+}$, $>MgHCO_3^-$, $>MgCO_3$. These species are calculated by mass conservation equation. These reactions are used for 25°C and 130°C. Equilibrium constant for each reaction changes as concentration changes. Equilibrium constants for reactions at 130°C are calculated using Van't Hoff equation. It is given below.

$$\ln\left(\frac{K_1}{K_2}\right) = -\left(\frac{\Delta H}{R}\right) \cdot \left(\frac{1}{T_2} - \frac{1}{T_1}\right)$$

where, Δ_H is enthalpy change (J/mol). T_1 and T_2 are temperatures. R is molar gas constant. The reaction network is shown below.

Log K values at different temperatures such as 60, 90, 130 and 170°C were calculated using above mentioned Van't Hoff equation. Log K values at 110°C were used as reference (T_2) to get enthalpy change. Using same enthalpy change, log K values at

different temperatures were calculated. Log K gives logarithmic value of K_{eq} which is equilibrium constant.

Table 2.1. Reactions for calcite and dolomite surface. Reactions (1 to 5,7,10) are for calcite, and reactions (6,8,9,11) for dolomite.

Reactions	Log K_{eq} (25°C)	Log K_{eq} (110°C)
$>CaOH + H^+ \leftrightarrow >CaOH^{2+}$	11.80	11.80
$>CaOH^{2+} + SO_4^{2-} \leftrightarrow >CaSO_4^- + H_2O$	-2.10	-3.25
$>CaOH + CO_3^{2-} \leftrightarrow >CaCO_3^- + H^+$	17.5	15.4
$>CO_3H \leftrightarrow >CO_3^- + H^+$	-5.10	-5.10
$>CO_3Ca^+ \leftrightarrow >CO_3^- + Ca^{2+}$	-2.6	-3.40
$>CO_3Mg^+ \leftrightarrow >CO_3^- + Mg^{2+}$	-2.6	-3.40
$>CaOH + CO_3^{2-} + H^+ \leftrightarrow >CaHCO_3^- + H_2O$	23.5	21.5
$>MgOH + CO_3^{2-} + H^+ \leftrightarrow >MgHCO_3^- + H_2O$	23.5	21.5
$>MgOH + CO_3^{2-} \leftrightarrow >MgCO_3^- + H^+$	15.4	17.5
$>CaO^- + H^+ \leftrightarrow >CaOH$	-12	-11
$>MgO^- + H^+ \leftrightarrow >MgOH$	-12	-11

*Log K values for reactions 1,2,4,5 and 6 are taken from Qiao et al., (2015). Log K values for 7 to 11 are taken from Pokrovsky et al., (1999). Log K for reactions 7-11 (where log K for 110°C is not available) were tuned to match the data.

3 RESULTS AND DISCUSSION

3.1 BASE CASE SIMULATIONS

Low salinity waterflooding experiments were mostly conducted using coreflooding techniques. For this work, data from Zhang et al., (2007) was used. Their experiments were carried out for different temperatures to understand effect of temperature on potential determining ions.

The experiments from Zhang et al., (2007) used homogeneous Stevns Klint chalk cores. The porosity was in the range of 45% to 50%. Permeability was in the range of 2mD to 5mD. Specific surface area was approximately $2\text{m}^2/\text{g}$. These cores, after drilling, were dried at 120°C and were cut to correct diameter (approximately 37mm) and length (approximately 70mm). The cores were saturated with two different brines. At first, cores were saturated with brine 1, which is formation water brine. Then brine 2 was injected at 25°C and 130°C at constant pH of 8.4. Compositions of brine 1 and brine 2 are shown below. This brine composition data and chalk core data from Zhang et al., (2007) was used in Crunchflow. The data mentioned in Crunchflow is shown below in table 3.2.

Chalk cores used for experiments from Zhang et al., (2007), were 7cm long and had diameter of 3.7 cm. For reactive transport modeling, it was assumed that water moves through 2-D column. Grid block of 75X25 was created with each grid having length and width of 0.1cm. Cores used in experiments as well as grid block created in Crunchflow are shown below.

Table 3.1. Composition of brine 1 and brine 2.

	Brine 1(mol/l)	Brine 2 (mol/l)
Na^+	0.573	0.504
K^+	-	-
Mg^{2+}	-	0.013
Ca^{2+}	-	0.013
Cl^-	-	0.556
HCO_3^-	-	-
SO_4^{2-}	-	0.013
SCN^-	0.573	0.573

Table 3.2. Parameters used in Crunchflow.

Parameter	Units	Value
Specific surface area of calcite	(m ² /g)	0.504
Specific surface area of dolomite ⁺	(m ² /g)	-
Diffusion Coefficient	(m ² /s)	1.7X10 ⁻⁸
Temperature	°C	25, 130
Porosity	%	0.556
pH	-	8.4
Dispersivity	cm	0.026

3.2 CHEMICAL ANALYSIS

After cores were saturated with formation water, seawater was injected. A pre-programmed Spectroquant Nova 60 photometer was used to determine the concentrations of Ca^{2+} and Mg^{2+} . Fig 3.1 shows concentrations of SCN^- , Ca^{2+} and Mg^{2+} after flooding brine 2 at 25°C from experiments. The dotted lines are values from simulation. Matching SCN^- curve from experiments and simulation indicates that flow conditions are successfully achieved in Crunchflow.

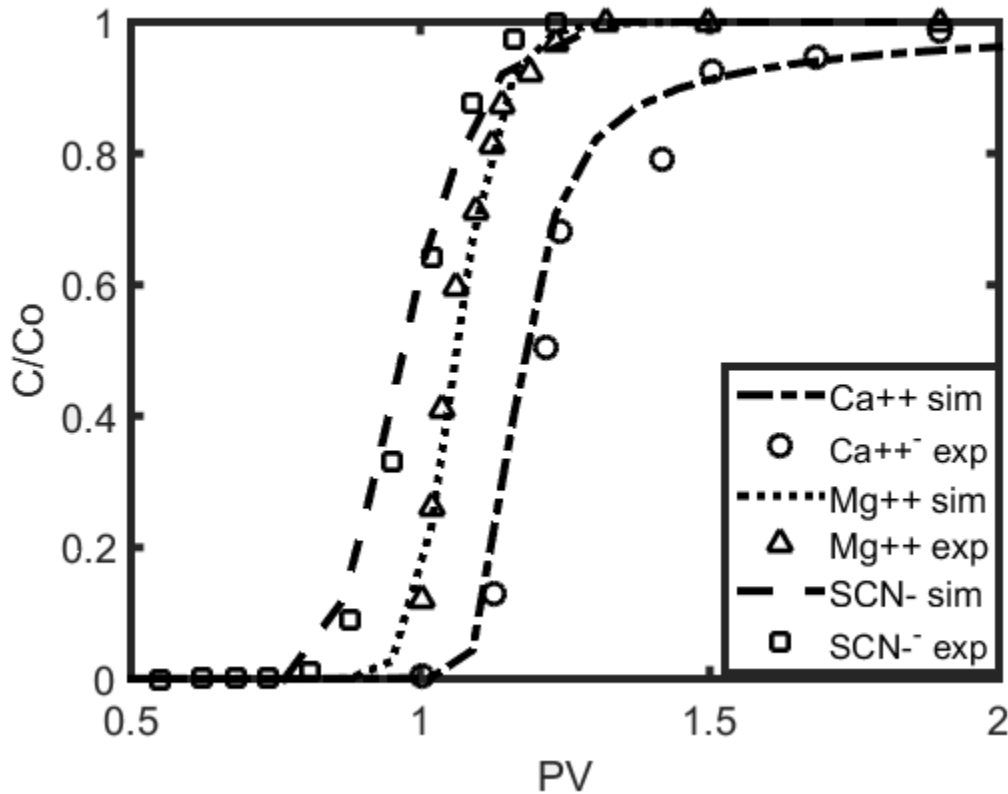


Fig 3.1. Concentrations of effluent Ca^{2+} , Mg^{2+} and SCN^- . Cores were already saturated with brine 1 at 25°C (Zhang et al., 2007). Dotted lines indicate values plotted from simulation.

SCN^- also known as Thiocyanate, is tracer used for reference during coreflooding, and is non-reactive. At 25°C, both Ca^{2+} and Mg^{2+} curves from Fig 3.1 are close to SCN^-

curve. This indicates that both ions are adsorbed or desorbed in lesser amount. Finally, all concentrations try to reach at initial concentration (equilibrium) at approximately 1.5 PV. The initial concentration of Ca^{2+} , Mg^{2+} and SCN^- were all 0.013 mol/l. The Mg^{2+} curve to immediate right of SCN^- curve shows that it is adsorbed on the rock surface but in lesser extent as compared to Ca^{2+} (as Ca^{2+} curve is to the extreme left).

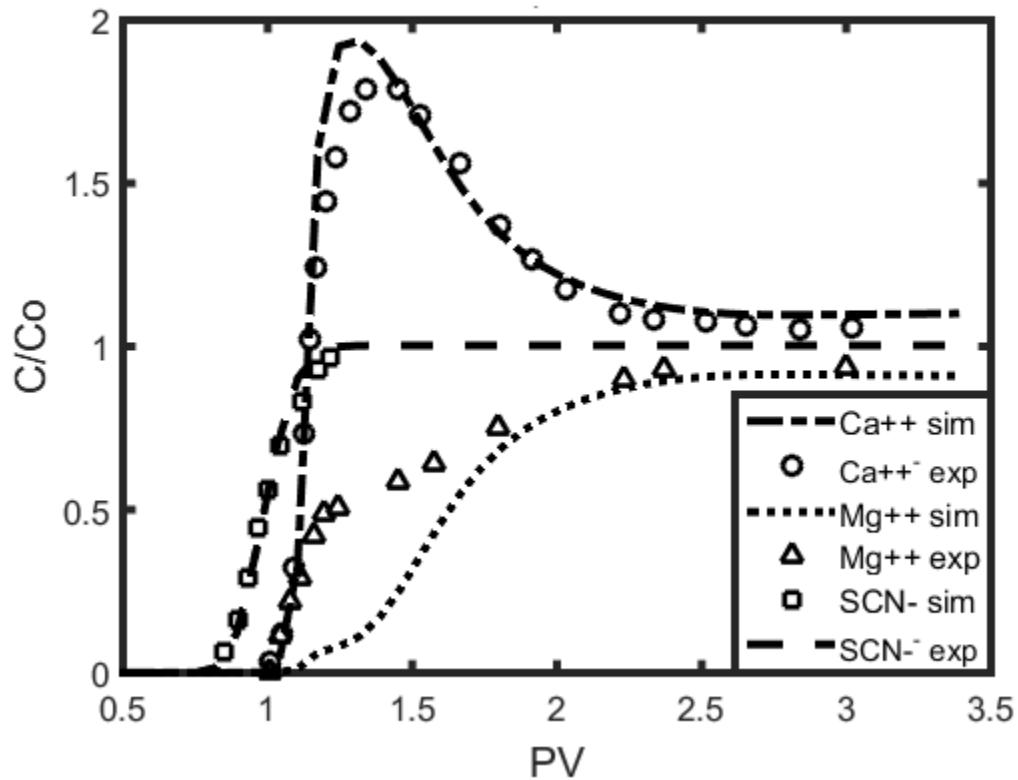


Fig 3.2. Concentrations of effluent Ca^{2+} , Mg^{2+} and SCN^- . Cores were already saturated with brine 1 at 130°C (Zhang et al., 2007). Dotted lines indicate values plotted from simulation.

Similarly, coreflooding test was carried out at 130°C. It showed significant difference in behavior of both ions. Fig 3.2 shows that Ca^{2+} concentration was suddenly spiked at 1 PV. The effluent concentration was almost double of initial concentration of Ca^{2+} . This means that additional Ca^{2+} from the rock surface was dissolved into effluent

concentration. Similarly, Mg^{2+} curve is showing less effluent concentration values than the initial concentration till 2PV was flooded. This suggests that Mg^{2+} from initial injected concentration is reacting on the rock surface. This reaction where Ca^{2+} is replaced by Mg^{2+} is known as dolomitization reaction. It leads to formation of dolomite. Higher temperature is favorable condition for this reaction.

3.3 SURFACE COMPLEXES

In order to understand wettability alteration, role of active surface sites is very important. These surface sites lead to reactions known as surface reactions. It is necessary to consider surface complexation modeling to simulate more accurate environment for wettability alteration. This section includes results from surface complexation model. Fig 3.3 shows surface complexes distribution.

Calcite rock surface has reactive surface sites such as >CO_3^- and >Ca^+ . Injecting additional concentration of different ions results in reaction of these ions with these sites. Reactions of surface sites and ions were discussed in section 2 including table 2.1. Thus, the surface sites concentrations may increase or decrease over time.

Fig 3.3 shows surface complexes distribution at 130°C . It can be noticed here that many sites are showing change in their concentration over PV injected. This concludes that for same injected brine, surface complexes concentrations change significantly showing reactions favor higher temperature. $\text{>CO}_3\text{H}$ concentration drops rapidly, and >CO_3^- and $\text{>CO}_3\text{Mg}^+$ concentrations increased over injected PV. This suggests that $\text{>CO}_3\text{H}$ detaches H^+ and becomes >CO_3^- and attracts Mg^{2+} . The reaction of >CO_3^- and Mg^{2+} forms $\text{>CO}_3\text{Mg}^+$. Hence, concentration of $\text{>CO}_3\text{Mg}^+$ increases.

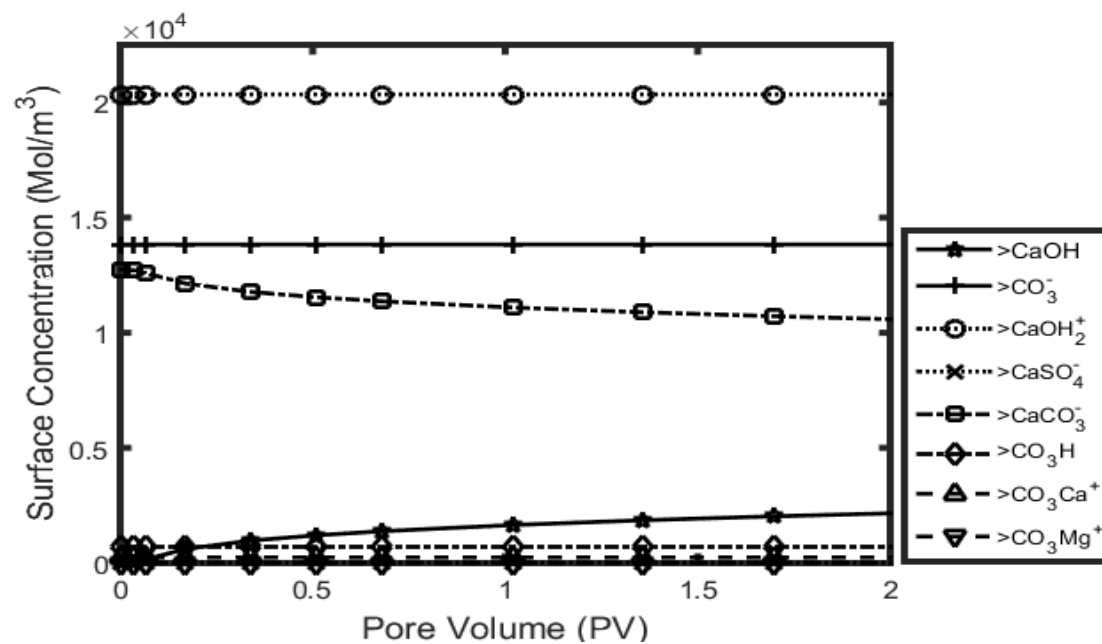


Fig 3.3. Surface complexes distribution at 25°C.

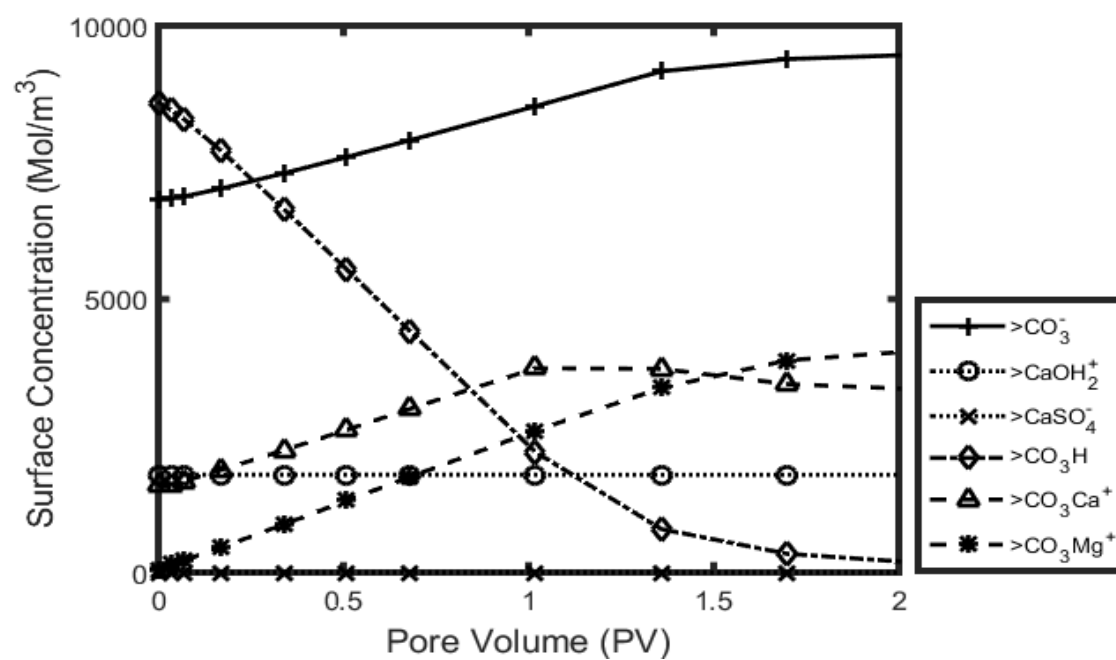


Fig 3.4. Surface complexes distribution at 130°C.

Figs 3.5 and 3.6 show surface concentration divided by initial surface concentration. This gives idea about how surface concentration changed from initial concentration over injected PV.

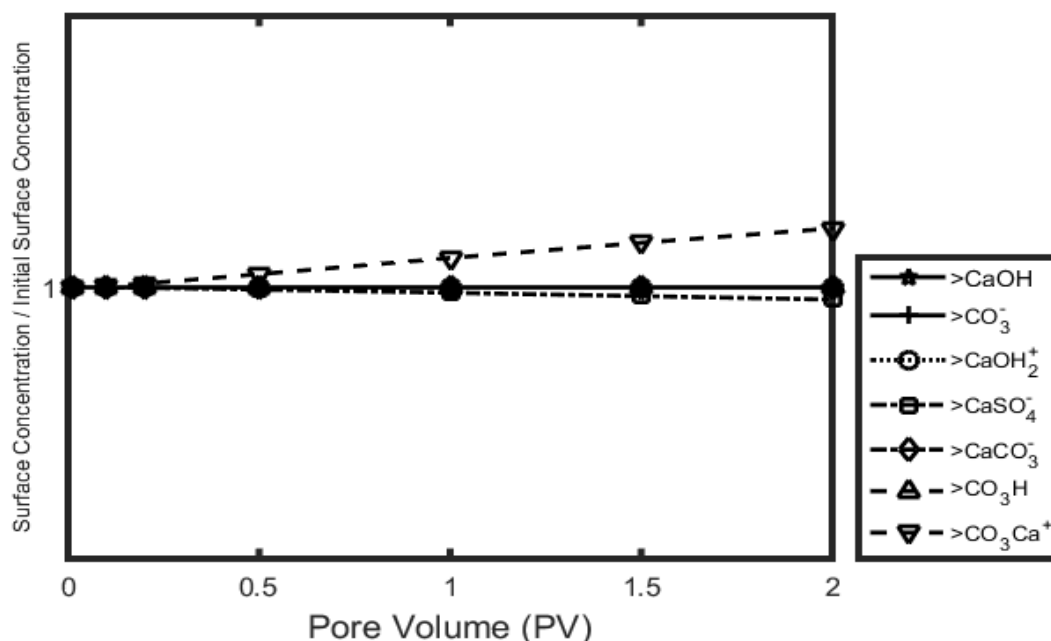


Fig 3.5. concentration ratio of surface complexes vs injected pore volume at 25°C.

3.4 EFFECT OF VARYING TEMPERATURE

To understand the effect of varying temperatures on adsorption and desorption of various ions and surface sites concentrations, simulations were run for 60 and 150°C. The effect of temperatures on chemical analysis are shown below in Fig 3.7 and 3.8.

It can be seen here that as the temperature increases more Ca^{2+} is getting desorbed from the surface of chalk. This additional desorbed Ca^{2+} may be from surface sites such as $>\text{CaOH}$, $>\text{CaOH}^{2+}$, $>\text{CaCO}_3^-$ and $>\text{CaSO}_4^-$.

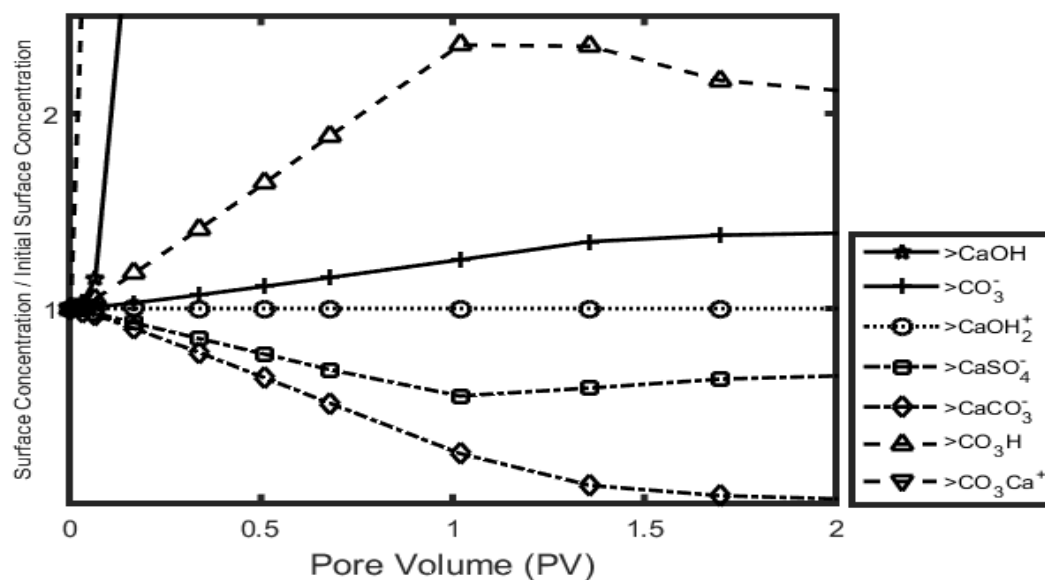


Fig 3.6. concentration ratio of surface complexes vs injected pore volume at 130°C.

Fig 3.8 shows chemical analysis of Mg^{2+} . It also shows progressive increase in adsorption, as the temperature increases. This also confirms that higher temperature favors dolomitization reaction.

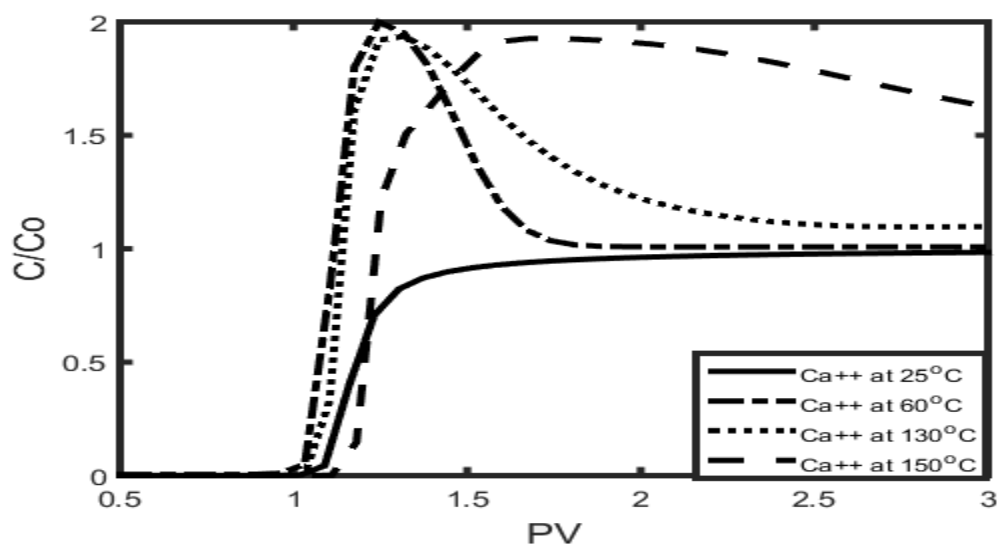


Fig 3.7. Chemical analysis of Ca^{2+} at 25, 60, 130, 150°C.

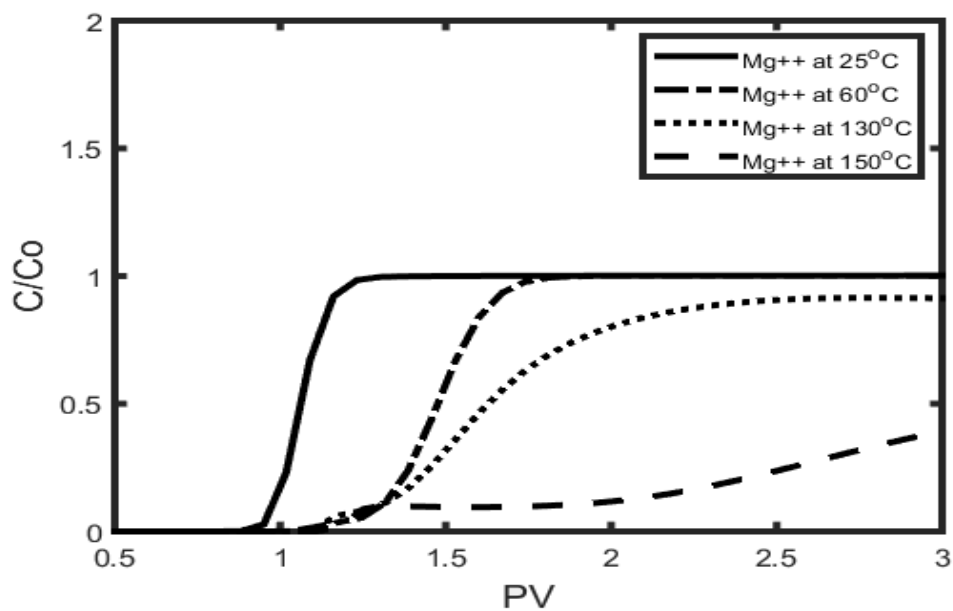


Fig 3.8. Chemical analysis of Ca^{2+} at 25,60,130,150°C.

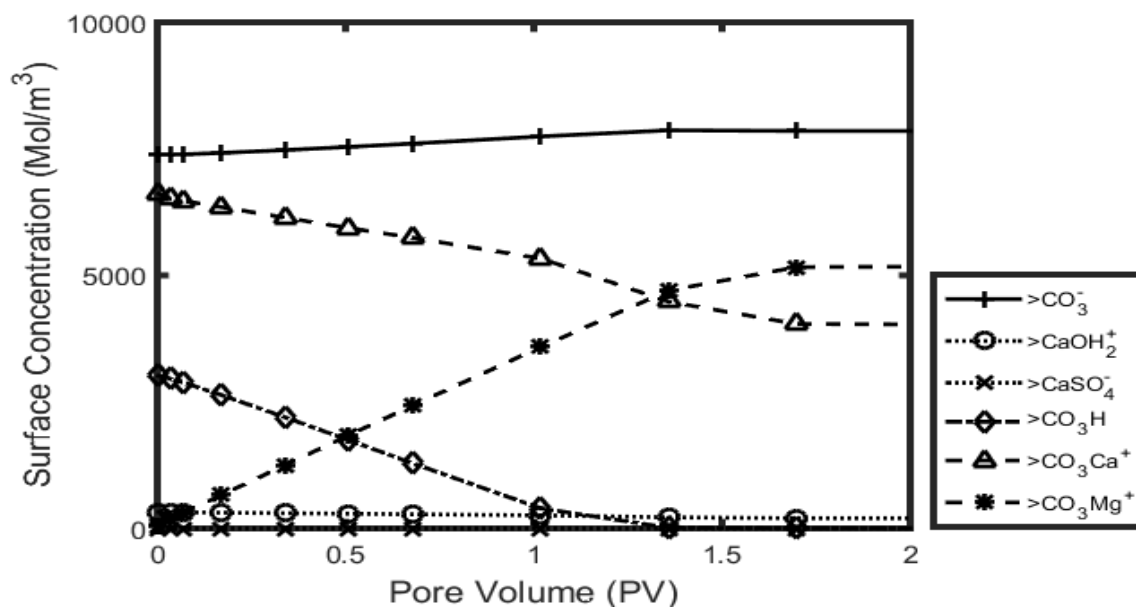


Fig 3.9. concentration ratio of surface complexes vs injected pore volume at 60°C.

Similarly, effect of varying temperatures on surface complexes was studied. Surface complexes distribution showed different trend for each temperature. Figs 3.9 and 3.10 show surface complexes concentration change.

It can be seen here that the increase in temperature from 25 to 60°C resulted all surface sites concentration change except $>\text{CaSO}_4^-$ and $>\text{CaOH}^{2+}$. It also shows that Mg^{2+} is more reactive towards $>\text{CO}_3^-$ than Ca^{2+} .

Finally, at 150°C, Mg^{2+} stops reacting with surface sites. Again, Ca^{2+} shows significant affinity towards $>\text{CO}_3\text{Ca}^+$.

Concentration ratios vs PV injected plots give better idea about change in concentration from initial concentration. They are shown below in Figs 3.11 and 3.12

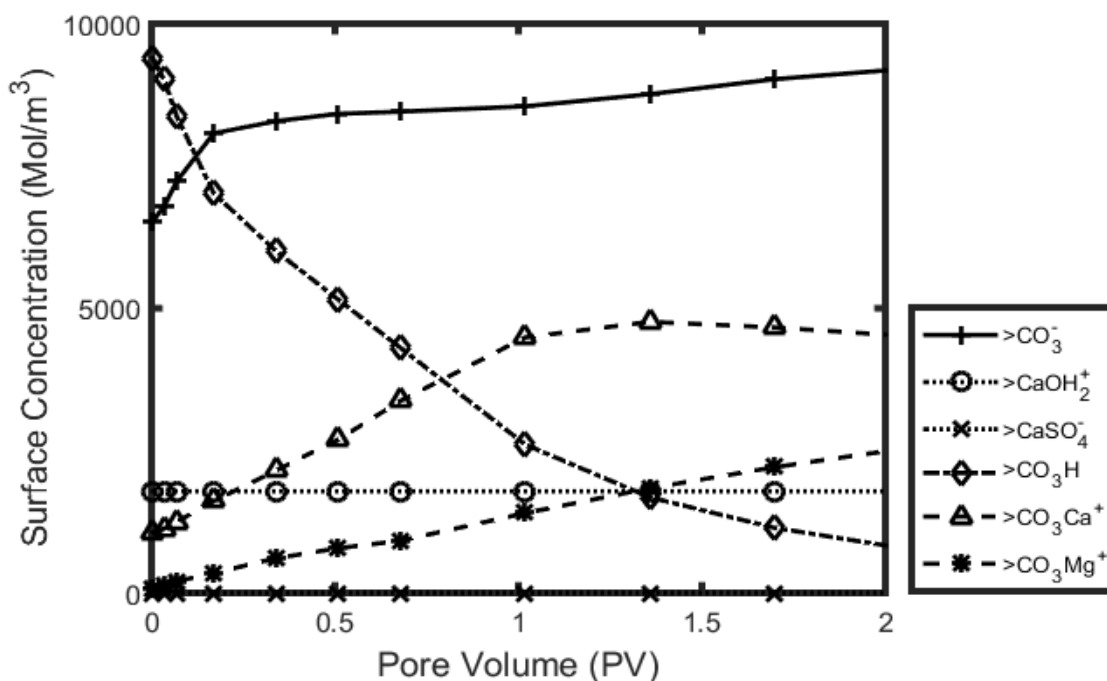


Fig 3.10. Concentration ratio of surface complexes vs injected pore volume at 150°C.

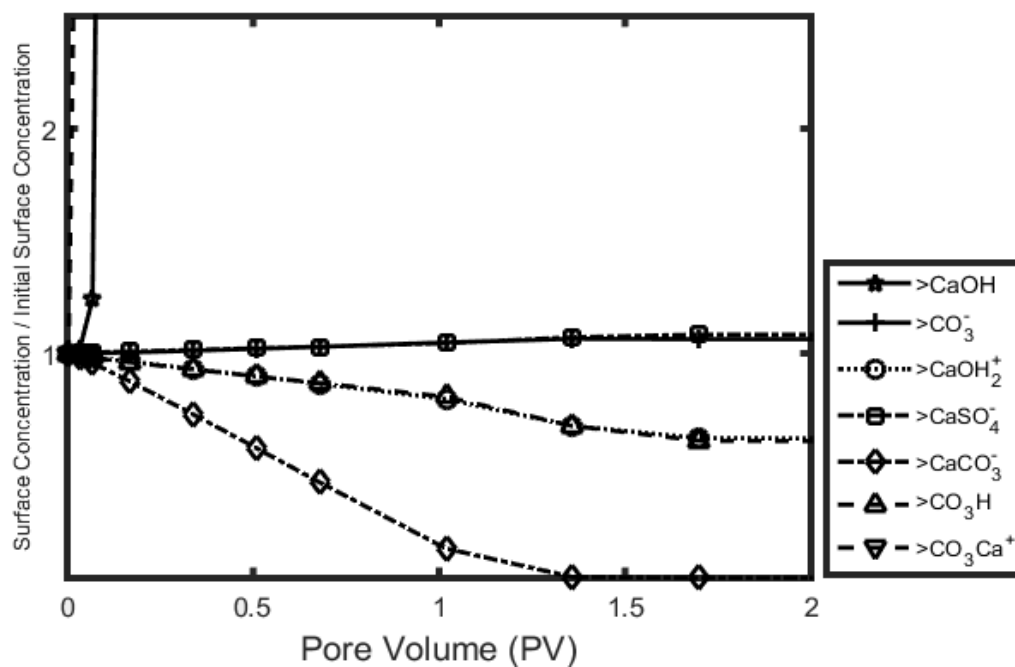


Fig 3.11. Concentration ratio of surface complexes vs injected pore volume at 60°C.

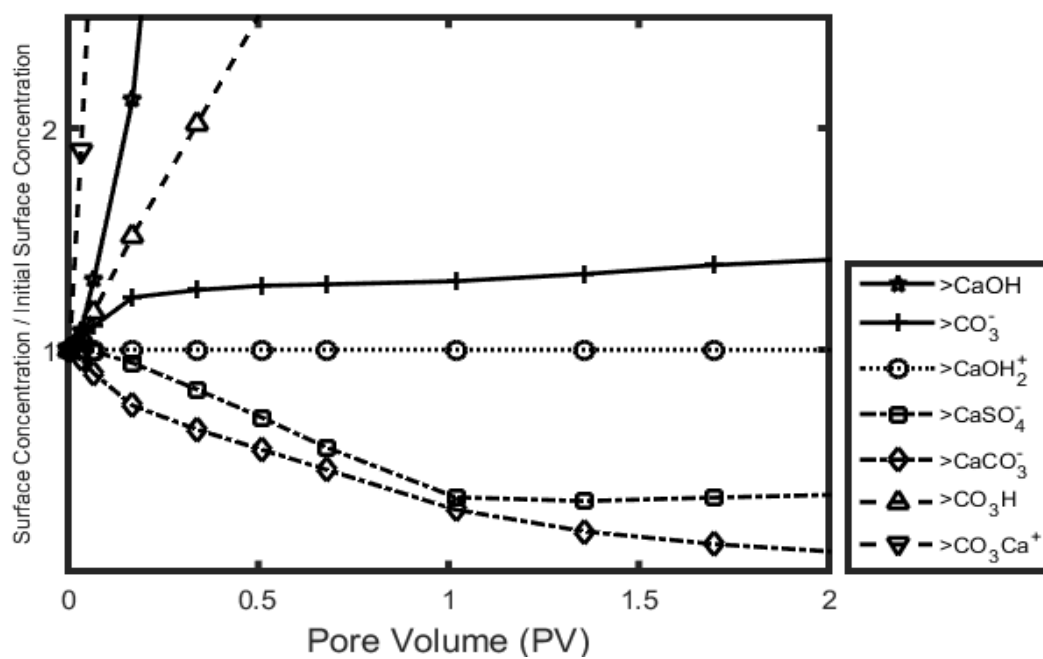


Fig 3.12. Concentration ratio of surface complexes vs injected pore volume at 150°C.

Fig 3.11 and 3.12 shows how surface sites deviate from their initial concentrations with respect to increasing injected PV. It can be noticed here that $>\text{CO}_3\text{H}$, $>\text{CO}_3^-$ and $>\text{CO}_3\text{Ca}^+$ show significant increase in 130 and 150°C. $>\text{CaSO}_4^-$ and $>\text{CaCO}_3^-$ are decreasing. This decrease in negative sites and increase in positive sites can result in significant wettability alteration.

To compare the increase in positively charged sites and decrease in negatively charged surface sites, ratio of each positively charged site concentration to its initial concentration and ratio each negatively charged surface site concentration to its initial concentration was plotted for different temperatures. These results are shown in Figs 3.13, 3.14 and 3.15. It can be seen here that at higher temperature concentration of $>\text{CO}_3\text{Ca}^+$ increased except at 60°C. At 150°C, $>\text{CO}_3\text{Ca}^+$ concentration increased approximately 4.2 times of initial concentration.

Previous study showed that Mg^{++} replaces Ca^{++} at elevated temperatures. Hence, ratio of concentrations of $>\text{CO}_3\text{Mg}^+$ to its initial concentration was plotted for different temperatures as shown in Fig 3.14. It shows that $>\text{CO}_3\text{Mg}^+$ concentration increased to much higher value than its initial concentration for 60°C. It was approximately 120 times greater than initial concentration. But, as the temperature increased, concentration change showed opposite trend. The ratio started decreasing. At 130°C, ratio is 70, and at 150°C, ratio is approximately 38. Even though ratio for $>\text{CO}_3\text{Mg}^+$ decreases, it is still much higher than ratio of $>\text{CO}_3\text{Ca}^+$ at any temperature. This indicates that Mg^{++} has higher affinity towards rock surface than Ca^{++} .

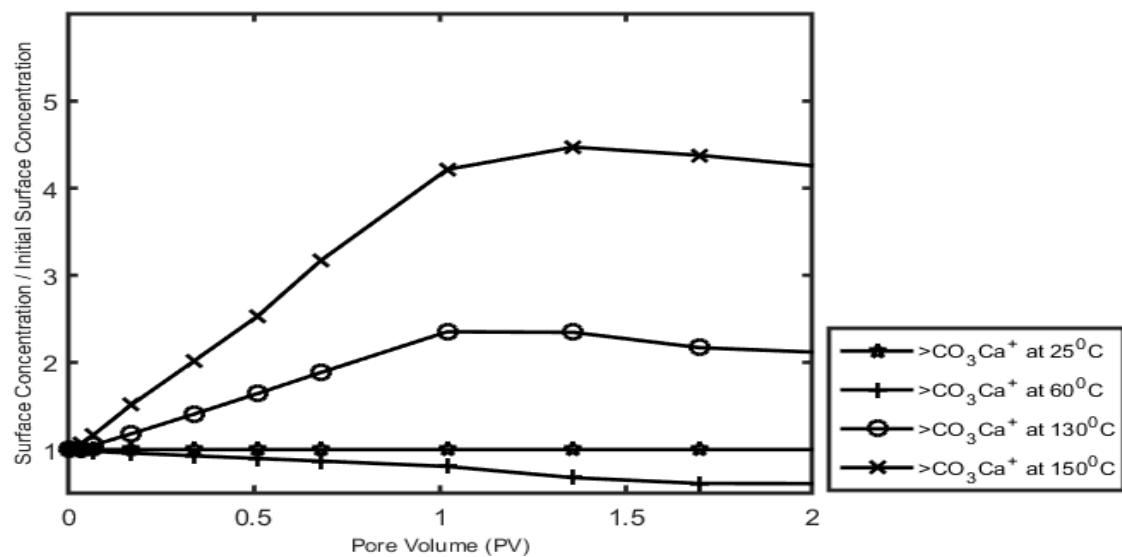


Fig 3.13. concentration ratio of $>\text{CO}_3\text{Ca}^+$ vs injected pore volume.

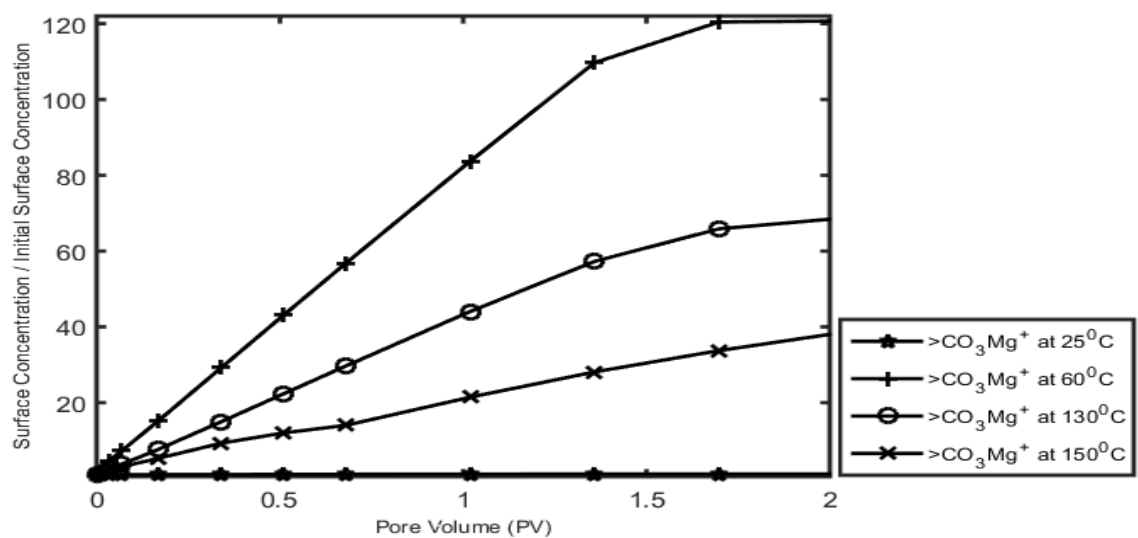


Fig 3.14. Concentration ratio of $>\text{CO}_3\text{Mg}^+$ vs injected pore volume.

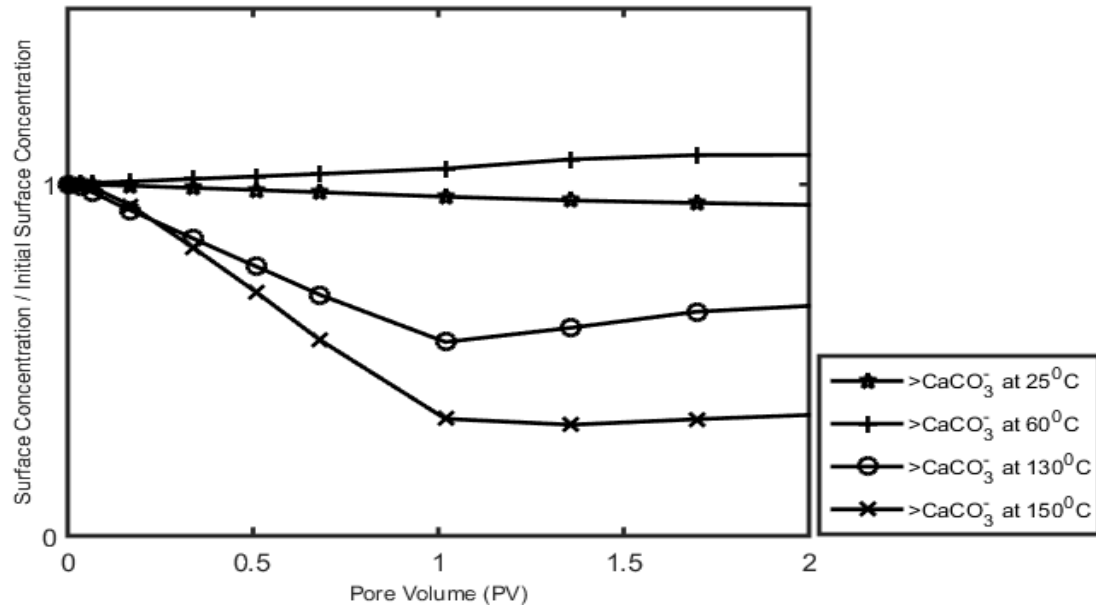


Fig 3.15. Concentration ratio of $>\text{CaCO}_3^-$ vs injected pore volume.

Thus, at higher temperature, Mg^{++} can act as main potential determining ion and can make greater contribution towards wettability alteration. Hence, increasing Mg^{++} in injecting brine for higher temperature, might increase the concentration of $>\text{CO}_3\text{Mg}^+$ at elevated temperature and can result in significant wettability alteration which can ultimately result in improved oil recovery.

On the other hand, overall charge on the rock surface determines whether water film will be stable or will collapse (Hiorth et al., 2010). Oil has negative surface potential. If rock has negative surface potential, water film will be more stable and it will be water wet. But, if rock is positively charged, water film will collapse and the surface will be oil-wet. Hence, it is important to have overall negative charge on the rock surface. When brine containing positive and negatively charged ions is injected, positively charged ions strip out negatively charged oil and negatively charged ions from brine attached to rock surface making it negative or reduce the positive charge.

In case of 25°C, total concentration of negatively charged sites was less than positively charged sites. Thus, overall rock surface was positively charged. When the temperature increased to 60°C, concentration of $>\text{CO}_3^-$ was increased significantly than any other positive sites. So, the total concentration of negatively charged sites was nearly equal to positively charged sites making surface charge less positive. It means that due to less positive charge on the rock surface, lesser oil will be attached to rock surface. As the temperature increased to 130°C and 150°C, $>\text{CO}_3\text{Mg}^+$ concentration was decreased reducing overall positively charged sites concentration and that reduced positive charge on the surface. Table 3.2 shows all surface sites concentrations at different temperatures.

Table 3.3. Surface sites concentration ratios at different temperatures.

Surface sites	At 25°C	At 60°C	At 130°C	At 150°C
$>\text{CO}_3\text{Mg}^+$	1.16	120.51	68.8	39.4
$>\text{CO}_3\text{Ca}^+$	1.00	0.61	2.11	4.23
$>\text{CaCO}_3^-$	0.93	1.01	0.70	0.39

Table 3.1 shows that total positive sites concentration goes on decreasing as temperature increases. $>\text{CaCO}_3^-$ is negative site which shows increase in concentration at 60°C and 130°C but then slightly decreases at 150°C.

It can be seen here that even though Mg^{++} has greater affinity towards rock surface, its affinity towards negatively charged sites on the rock surface decreased with increased temperature. This resulted into decreasing concentration of $>\text{CO}_3\text{Mg}^+$. This suggests that Mg^{++} reacting on rock surface to precipitate as magnesium rich mineral dolomite. At the

same time, Ca^{++} showed less affinity towards rock surface and Ca^{++} concentration from effluent was higher than initial injected concentration of Ca^{++} . This indicates that excess Ca^{++} from effluent came from dissolution of calcite. To verify, dolomite precipitation and calcite dissolution were calculated.

Table 3.4. Mineral fractions at different temperatures.

Minerals	At 25°C	At 60°C	At 130°C	At 150°C
	fraction	fraction	fraction	fraction
Calcite	1	1	0.998	0.997
Dolomite	1.16	0.991	1.86	8.174

3.5 BRINE COMPOSITION AND CALCITE DISSOLUTION

To understand relation between brine composition and calcite dissolution, several simulations were run using different brine compositions. Oil recovery percentages and brine compositions are used to relate them with the calcite dissolution. It was found that oil recovery and calcite dissolution increased with increase in volume. Following table shows the relation between brine composition, calcite dissolution and oil recovery percentage. This shows that there is correlation between all three of them.

Table 3.5. Oil recovery percentage and calcite dissolution relation.

Ca ⁺⁺ (Mol/L)	Mg ⁺⁺ (Mol/L)	SO ₄ ²⁻ (Mol/L)	Temp (°C)	Oil recovery (%)	Calcite dissolved (Vol %)_
0.013	0.0445	0.000	70°C	9	0.0001785
0.013	0.0445	0.000	130°C	51.5	0.0431
0.013	0.0445	0.024	70°C	9	0.0000838
0.013	0.0445	0.024	130°C	26	0.0219
0.013	0.0445	0.048	70°C	9	0.0001411
0.013	0.0445	0.048	130°C	29	0.0351
0.013	0.0945	0.096	70°C	9	0.0002150
0.013	0.0945	0.096	130°C	61	0.0805

4 CONCLUSION AND RECOMMENDATION

4.1 CONCLUSION

This study presents reactive transport model for high salinity waterflooding for carbonate. Surface complexation modeling was also part of this study. Surface complexation model helped to understand surface sites concentration changes with respect to different temperatures. Oil recovery mechanism based on water chemistry was studied using this model.

Based on chemical analysis at 25°C, Ca^{++} from injecting brine showed more affinity towards rock surface than Mg^{++} . At 130°C, Mg^{++} was more reactive towards rock surface than Ca^{++} . Surface sites also showed significant changes in concentration at different temperatures. It showed that both $>\text{CO}_3\text{Ca}^+$ and $>\text{CO}_3\text{Mg}^+$ concentrations decrease with increase in temperature. $>\text{CO}_3^-$ concentration showed accordance with increasing temperature and improved oil recovery by reducing positive charge on the rock surface.

Thus, the excess Mg^{++} , which reacted on rock surface, resulted in precipitation of dolomite. Hence, excess Ca^{++} from the calcite in effluent concentration in chemical analysis was result of calcite dissolution. Calcite dissolution is supposed to enhanced by organic matter attached to it. Thus, calcite dissolution is plausible reason for improved oil recovery.

Also, at 130 and 150°C, $>\text{CO}_3\text{Mg}^+$ and $>\text{CO}_3\text{Ca}^+$ concentrations were less compared to 25 and 60°C. It means surface potential at 25 and 60°C was highly positive than at 130°C and 150°C. Initially less positive surface potential of rock reduces attraction between rock surface and negative carboxylic group from oil. This reduced binding of rock and oil group helps to change the wettability of rock during waterflooding.

4.2 RECOMMENDATIONS

Since, reactions related to mineral dissolution depend on reaction rates, and surface site reactions depend on equilibrium constants, it is necessary to have accurate values of both from experimental data in order to simulate exact reaction environment. This study was only based on water-rock interaction.

Carboxylic group which is present in oil was not considered in model. To understand water-oil-rock interaction, -COO (carboxylic group) must be considered in model. It can help to understand relation between oil recovery and surface complexation and mineral dissolution mechanism.

BILBIOGRAPHY

1. Abdallah, W., et al. (1986). "Fundamentals of wettability." *Technology* 38(1125-1144): 268.
2. Agbalaka, C. C., et al. (2009). "Coreflooding studies to evaluate the impact of salinity and wettability on oil recovery efficiency." *Transport in porous media* 76(1): 77-94.
3. Ahsan, R. and I. L. Fabricius (2010). Sorption of magnesium and sulfate ions on calcite. 72nd EAGE Conference and Exhibition incorporating SPE EUROPEC 2010.
4. Al-Shalabi, E. W., et al. (2014). A Fundamental Model for Predicting Oil Recovery Due to Low Salinity Water Injection in Carbonate Rocks, Society of Petroleum Engineers.
5. Al Harrasi, A., et al. (2012). Laboratory investigation of low salinity waterflooding for carbonate reservoirs. Abu Dhabi International Petroleum Conference and Exhibition, Society of Petroleum Engineers.
6. Alotaibi, M. B., et al. (2010). Wettability challenges in carbonate reservoirs. SPE Improved Oil Recovery Symposium, Society of Petroleum Engineers.
7. Alvarado, V. and E. Manrique (2010). "Enhanced oil recovery: an update review." *Energies* 3(9): 1529-1575.
8. Austad, T. (2013). "Water-Based EOR in Carbonates and Sandstones: New Chemical Understanding of the EOR Potential Using Smart Water." *Enhanced Oil Recovery Field Case Studies*: 301-335.
9. Austad, T., et al. (2011). "Conditions for a low-salinity enhanced oil recovery (EOR) effect in carbonate oil reservoirs." *Energy & fuels* 26(1): 569-575.
10. Austad, T., et al. (2005). Seawater as IOR fluid in fractured chalk. SPE International Symposium on Oilfield Chemistry, Society of Petroleum Engineers.

11. Bagci, S., et al. (2001). "Effect of brine composition on oil recovery by waterflooding." *Petroleum science and technology* 19(3-4): 359-372.
12. Brady, P. V. and J. L. Krumhansl (2012). "A surface complexation model of oil–brine–sandstone interfaces at 100° C: Low salinity waterflooding." *Journal of Petroleum Science and Engineering* 81: 171-176.
13. Chandrasekhar, S. (2013). "Wettability alteration with brine composition in high temperature carbonate reservoirs."
14. Chou, L., et al. (1989). "Comparative study of the kinetics and mechanisms of dissolution of carbonate minerals." *Chemical Geology* 78(3): 269-282.
15. Cuiec, L. (1984). Rock/crude-oil interactions and wettability: An attempt to understand their interrelation. SPE Annual Technical Conference and Exhibition, Society of Petroleum Engineers.
16. Dake, L. P. (1983). *Fundamentals of reservoir engineering*, Elsevier.
17. Fathi, S. J., et al. (2010). "'Smart Water' as a Wettability Modifier in Chalk: The Effect of Salinity and Ionic Composition." *Energy & fuels* 24(4): 2514-2519.
18. Fathi, S. J., et al. (2011). "Effect of water-extractable carboxylic acids in crude oil on wettability in carbonates." *Energy & fuels* 25(6): 2587-2592.
19. Fathi, S. J., et al. (2011). "Water-based enhanced oil recovery (EOR) by "smart water": Optimal ionic composition for EOR in carbonates." *Energy and Fuels* 25(11): 5173-5179.
20. Heidari, P. and L. Li (2014). "Solute transport in low-heterogeneity sand boxes: The role of correlation length and permeability variance." *Water Resources Research* 50(10): 8240-8264.
21. Hill, D. (1984). "Diffusion coefficients of nitrate, chloride, sulphate and water in cracked and uncracked Chalk." *Journal of soil science* 35(1): 27-33.

22. Hiorth, A., et al. (2010). "The impact of pore water chemistry on carbonate surface charge and oil wettability." *Transport in porous media* **85**(1): 1-21.
23. Hognesen, E. J., et al. (2005). Waterflooding of preferential oil-wet carbonates: Oil recovery related to reservoir temperature and brine composition. SPE Europec/EAGE Annual Conference, Society of Petroleum Engineers.
24. Jiang, H., et al. (2014). Lab observation of low salinity waterflooding for a phosphoria reservoir rock. SPE Western North American and Rocky Mountain Joint Meeting, Society of Petroleum Engineers.
25. Kafili Kasmaei, A. and D. Rao (2014). Is Wettability Alteration the Main Cause for Enhanced Recovery in Low-Salinity Waterflooding? SPE Improved Oil Recovery Symposium, Society of Petroleum Engineers.
26. Kafili Kasmaei, A. and D. N. Rao (2015). "Is Wettability Alteration the Main Cause for Enhanced Recovery in Low-Salinity Waterflooding?" *SPE Reservoir Evaluation & Engineering* **18**(02): 228-235.
27. Lager, A., et al. (2008). "Low Salinity Oil Recovery - An Experimental Investigation1."
28. Lager, A., et al. (2008). LoSal Enhanced Oil Recovery: Evidence of Enhanced Oil Recovery at the Reservoir Scale, Society of Petroleum Engineers.
29. Madland, M., et al. (2011). "Chemical alterations induced by rock–fluid interactions when injecting brines in high porosity chalks." *Transport in porous media* **87**(3): 679-702.
30. McGuire, P. L., et al. (2005). Low salinity oil recovery: An exciting new EOR opportunity for Alaska's north slope. SPE Western Regional Meeting, Proceedings.
31. Pokrovsky, O. and J. Schott (2002). "Surface chemistry and dissolution kinetics of divalent metal carbonates." *Environmental science & technology* **36**(3): 426-432.

32. Qiao, C., et al. (2015). Modeling Low Salinity Waterflooding in Mineralogically Different Carbonates. SPE Annual Technical Conference and Exhibition, Society of Petroleum Engineers.
33. Qiao, C., et al. (2014). A Mechanistic Model for Wettability Alteration by Chemically Tuned Water Flooding in Carbonate Reservoirs, Society of Petroleum Engineers.
34. Qiao, C., et al. (2015). "A Mechanistic Model for Wettability Alteration by Chemically Tuned Waterflooding in Carbonate Reservoirs." SPE Journal.
35. Rao, D. N. (1996). Wettability effects in thermal recovery operations. SPE/DOE Improved Oil Recovery Symposium, Society of Petroleum Engineers.
36. RezaeiDoust, A., et al. (2009). "Smart water as wettability modifier in carbonate and sandstone: A discussion of similarities/differences in the chemical mechanisms." *Energy & fuels* **23**(9): 4479-4485.
37. Romanuka, J., et al. (2012). Low salinity EOR in carbonates. SPE Improved Oil Recovery Symposium, Society of Petroleum Engineers.
38. Shariatpanahi, S. F., et al. (2011). "Initial wetting properties of carbonate oil reservoirs: effect of the temperature and presence of sulfate in formation water." *Energy & fuels* **25**(7): 3021-3028.
39. Sheng, J. (2013). Enhanced oil recovery field case studies, Gulf Professional Publishing.
40. Shimoyama, A. and W. D. Johns (1972). "Formation of alkanes from fatty acids in the presence of CaCO_3 ." *Geochimica et Cosmochimica Acta* **36**(1): 87-91.
41. Speight, J. G. (1999). The desulfurization of heavy oils and residua, CRC Press.

VITA

Sameer Salasakar received his Bachelor of Science degree in Chemical engineering from University of Pune in June 2013. He joined Dr. Heidari's group at Petroleum Engineering department in February 2015 as a graduate student in Missouri University of Science and Technology. In July 2017, he received his Master degree in Petroleum Engineering from Missouri University of Science and Technology.